

transfusions die before TTI evaluation.²⁸ In fact, when we inquired about the outcomes of transfusions with components containing verified HBV at medical facilities, 99 (42%) of 238 patients who had been transfused with such components had already died (JRC data from 2009 to 2010). The transmissibility of ID-NAT-positive donations might require reevaluation because of the low numbers of patients analyzed in the previous study⁷ (30 and 22 for OBI- and WP-related cases, respectively). The fact that a large proportion of elderly patients are immune to HBV due to prior infection might also contribute to the low figure for established TT-HBV and, finally, anti-HBs in cotransfused components neutralizes HBV. Classified WP donation that is anti-HBs positive and could be attributed to possible vaccine breakthrough infection or anti-HBc-negative chronic OBI could also be a factor influencing infectivity. However, we have not encountered any implicated WP donations with anti-HBs among established TT-HBV infections.

Because of the high probability of a residual risk of TT-HBV, novel strategies that reinforce the safety of blood components but do not damage the blood supply should be implemented. Transfusion with ID-NAT-negative infectious components currently cause 15 and 25% of OBI- and WP-related TT-HBV infections, respectively (Table 2), and screening with ID-NAT would interdict 85 and 75% of these infections, respectively (Table 5). With respect to this, the ID-NAT screening of only donations with low anti-HBc and anti-HBs titers that are currently qualified has been suggested.²⁹ However, screening with ID-NAT might not be as effective as expected. For example, the variability in viral load in individuals with OBI might allow persistent OBI-related TT-HBV infection; some individuals might have an intermittently elevated viral load.³⁰⁻³³ Such donations could be identified as HBV positive only when the viral load exceeds the detection threshold of ID-NAT screening. Alternatively, the detection of intermittent viremia might reflect the stochastic phenomenon inherent in NAT technology, particularly at very low viral concentrations. Moreover, one report describes a donor in whom viral load increased in blood samples over a period of several years.³⁴ Nine among 48 blood donations from this donor were ID-NAT positive, and two of four ID-NAT-positive and three ID-NAT-negative blood transfusions had caused TT-HBV infections. The diverse fluctuation of viremia described above has supposedly hindered the efficient detection of viremic donations by pool-based NAT screening,³⁵ which is predictable even in the event of ID-NAT screening. Table 5 shows that ID-NAT is not sensitive enough in 16% of established OBI-related transmission events although most of those events are caused by FFP or PC transfusions and ID-NAT screened RBC transfusions are relatively safe. Moreover, although viremia is considered undetectable in most individuals with OBI, this assumption might be

dependent on the sensitivity of the NAT used; a considerable number of donations might have viremia with a viral load below the ID-NAT detection limit.

Another strategy that might increase the safety of OBI-derived donations could be to accept only those OBI-derived donations with a profile that is safer than the current standards, if such a profile can be found and systematically applied. We initially expected to find that OBI donations with a very low anti-HBc titer would be safer based on ID-NAT. However, the finding from the ID-NAT trial was that the frequency of viremia does not correlate with anti-HBc titers in the range of S/CO 1.0 to 11.9. Therefore, we concluded that the risk of TT-HBV infection will not be mitigated by implementing a strategy that qualifies only donations with very low anti-HBc titers such as S/CO between 1.0 and 3.0.

We speculated during 2003 that more than 4% of donations would be disqualified if the anti-HBc cutoff were set at 2¹, that is, if all donations with low anti-HBc and anti-HBs titers are rejected. We thought that the loss of so many donations would cause catastrophic damage to the blood inventory and thus that cutoff was not implemented. However, based on current data, the number of donations received in 2010 with low anti-HBc and anti-HBs titers was 69,000, which accounts for 1.31% of all donations in Japan. Given this ratio, we consider that to eliminate all donations with low anti-HBc and anti-HBs titers is feasible. We verified that severe hepatitis is caused more often by OBI- than WP-derived blood. The fact that two patients died of fulminant hepatitis related to OBI-related donations is also serious. Rejecting this category of donations would eliminate nearly all those harboring a risk of OBI-related infection.²⁶ However, a slight, but distinct risk of TT-HBV infection might persist because a small fraction of OBI donors have an anti-HBc titer of less than 1.0 S/CO, and these donors as well as NAT WP donors present a TT-HBV risk.³⁶ A committee of the Ministry of Health, Labour and Welfare of the Japanese government has just discussed and authorized the implementation of a new policy in which all donations with low anti-HBc and anti-HBs titers would be rejected.

In conclusion, ID-NAT screening of donations with low anti-HBc and anti-HBs titers revealed that nearly 2% of these donations were associated with low-level viremia and that viremia was identified over the entire range of anti-HBc titers. Importantly, anti-HBc titer did not correlate with the frequency of viremia. The elimination of all donations with low anti-HBc and anti-HBs titers would be important to any strategy aimed at preventing OBI-related TT-HBV infections in countries such as Japan that have a slightly elevated HBV prevalence in blood donations. If this strategy is implemented, the only acceptable donors with OBI in Japan will be those with high anti-HBs titers (≥ 200 IU/L).

ACKNOWLEDGMENT

All data presented herein were obtained by the staff at Japanese Red Cross blood centers who are engaged in blood testing, quality assurance, or liaison with medical facilities.

CONFLICT OF INTEREST

This research did not receive support in the form of grants, equipment, or drugs. The authors have no conflicts of interest regarding this article.

REFERENCES

1. Tanaka J, Koyama T, Mizui M, Uchida S, Katayama K, Matsuo J, Akita T, Nakashima A, Miyakawa Y, Yoshizawa H. Total numbers of undiagnosed carriers of hepatitis C and B viruses in Japan estimated by age- and area-specific prevalence on the national scale. *Intervirology* 2011;54:185-95.
2. Tanaka J, Kumagai J, Katayama K, Komiya Y, Mizui M, Yamanaka R, Suzuki K, Miyakawa Y, Yoshizawa H. Sex- and age-specific carriers of hepatitis B and C viruses in Japan estimated by the prevalence in the 3,485,648 first-time blood donors during 1995-2000. *Intervirology* 2004;47:32-40.
3. Ohnuma H, Tanaka T, Yoshikawa A, Murokawa H, Minegishi K, Yamanaka R, Iizuka HY, Miyamoto M, Satoh S, Nakahira S, Tomono T, Murozuka T, Takeda Y, Doi Y, Mine H, Yokoyama S, Hirose T, Nishioka K; Japanese Red Cross NAT Screening Research Group. The first large-scale nucleic acid amplification testing (NAT) of donated blood using multiplex reagent for simultaneous detection of HBV, HCV, and HIV-1 and significance of NAT for HBV. *Microbiol Immunol* 2001;45:667-72.
4. Allain JP. Occult hepatitis B virus infection: implications in transfusion. *Vox Sang* 2004;86:83-91.
5. Raimondo G, Allain JP, Brunetto MR, Buendia MA, Chen DS, Colombo M, Craxi A, Donato F, Ferrari C, Gaeta GB, Gerlich WH, Levrero M, Locarnini S, Michalak T, Mondelli MU, Pawlotsky JM, Pollicino T, Prati D, Puoti M, Samuel D, Shouval D, Smedile A, Squadrito G, Trépo C, Zoulim F, et al. Statements from the Taormina expert meeting on occult hepatitis B virus infection. *J Hepatol* 2008;49:652-7.
6. Mine H, Emura H, Miyamoto M, Tomono T, Minegishi K, Murokawa H, Yamanaka R, Yoshikawa A, Nishioka K; Japanese Red Cross NAT Research Group. High throughput screening of 16 million serologically negative blood donors for hepatitis B virus, hepatitis C virus and human immunodeficiency virus type-1 by nucleic acid amplification testing with specific and sensitive multiplex reagent in Japan. *J Virol Methods* 2003;112:145-51.
7. Satake M, Taira R, Yugi H, Hino S, Kanemitsu K, Ikeda H, Tadokoro K. Infectivity of blood components with low hepatitis B virus DNA levels identified in a lookback program. *Transfusion* 2007;47:1197-205.
8. Pharmaceutical and Food Safety Bureau, Blood and Blood Products Division. Guidelines for lookback study for blood products. Tokyo, Japan: Japanese Ministry of Health, Labour and Welfare; 2005. p. 2-26.
9. Busch MP, Glynn SA, Stramer SL, Strong DM, Caglioti S, Wright DJ, Pappalardo B, Kleinman SH; NHLBI-REDS NAT Study Group. A new strategy for estimating risks of transfusion-transmitted viral infections based on rates of detection of recently infected donors. *Transfusion* 2005;45:254-64.
10. Satake M. Infectious risks associated with the transfusion of blood components and pathogen inactivation in Japan. *Int J Hematol* 2004;80:306-10.
11. Yoshikawa A, Gotanda Y, Itabashi M, Minegishi K, Kanemitsu K, Nishioka K; Japanese Red Cross NAT Screening Research Group. HBV NAT positive [corrected] blood donors in the early and late stages of HBV infection: analyses of the window period and kinetics of HBV DNA. *Vox Sang* 2005;88:77-86.
12. Kosaka Y, Takase K, Kojima M, Shimizu M, Inoue K, Yoshida M, Tanaka S, Akahane Y, Okamoto H, Tsuda F, Miyakawa Y, Mayumi M. Fulminant hepatitis B: induction by hepatitis B virus mutants defective in the precore region and incapable of encoding e antigen. *Gastroenterology* 1991;100:1087-94.
13. Sato S, Suzuki K, Akahane Y, Akamatsu K, Akiyama K, Yunomura K, Tsuda F, Tanaka T, Okamoto H, Miyakawa Y, Mayumi M. Hepatitis B virus strains with mutations in the core promoter in patients with fulminant hepatitis. *Ann Intern Med* 1995;122:241-8.
14. Okamoto H, Yotsumoto S, Akahane Y, Yamanaka T, Miyazaki Y, Sugai Y, Tsuda F, Tanaka T, Miyakawa Y, Mayumi M. Hepatitis B viruses with precore region defects prevail in persistently infected hosts along with seroconversion to the antibody against e antigen. *J Virol* 1990;64:1298-303.
15. Kurosaki M, Enomoto N, Asahina Y, Sakuma I, Ikeda T, Tozuka S, Izumi N, Marumo F, Sato C. Mutations in the core promoter region of hepatitis B virus in patients with chronic hepatitis B. *J Med Virol* 1996;49:115-23.
16. Hoofnagle JH, Seeff LB, Bales ZB, Zimmerman HJ. Type B hepatitis after transfusion with blood containing antibody to hepatitis B core antigen. *N Engl J Med* 1978;298:1379-83.
17. Iizuka H, Ohmura K, Ishijima A, Satoh K, Tanaka T, Tsuda F, Okamoto H, Miyakawa Y, Mayumi M. Correlation between anti-HBc titers and HBV DNA in blood units without detectable HBsAg. *Vox Sang* 1992;63:107-11.
18. Japanese Red Cross Non-A, Non-B Hepatitis Research Group. Effect of screening for hepatitis C virus antibody and hepatitis B virus core antibody on incidence of post-transfusion hepatitis. *Lancet* 1991;338:1040-1.
19. Nozawa Y, Ohto H. An autopsy case of post-transfusion fulminant hepatitis B due to screened blood for anti-hepatitis B core. *Kanzo* 1993;34:433-6.

20. Klein HG, Anderson D, Bernardi MJ, Cable R, Carey W, Hoch JS, Robitaille N, Sivilotti ML, Smaill F. Pathogen inactivation: making decisions about new technologies. Report of a consensus conference. *Transfusion* 2007;47:2338-47.
21. McCullough J. Pathogen inactivation: a new paradigm for preventing transfusion-transmitted infections. *Am J Clin Pathol* 2007;128:945-55.
22. Allain JP, Hewitt PE, Tedder RS, Williamson LM. Evidence that anti-HBc but not HBV DNA testing may prevent some HBV transmission by transfusion. *Br J Haematol* 1999;107:186-95.
23. Grob P, Jilg W, Bornhak H, Gerken G, Gerlich W, Günther S, Hess G, Hüdig H, Kitchen A, Margolis H, Michel G, Trepo C, Will H, Zanetti A, Mushahwar I. Serological pattern "anti-HBc alone": report on a workshop. *J Med Virol* 2000;62:450-5.
24. Gerlich WH, Wagner FF, Chudy M, Harritshoj LH, Lattermann A, Wienzek S, Glebe D, Saniewski M, Schüttler CG, Wend UC, Willems WR, Bauerfeind U, Jork C, Bein G, Platz P, Ullum H, Dickmeiss E. HBsAg non-reactive HBV infection in blood donors: transmission and pathogenicity. *J Med Virol* 2007;79:S32-S36.
25. Dreier J, Kröger M, Diekmann J, Götting C, Kleesiek K. Intermittent HBV viremia in an anti-HBc and anti-HBs-positive blood donor. *Transfus Med* 2005;15:65-6.
26. Stramer SL, Zou S, Notari EP, Foster GA, Krysztof DE, Musavi F, Dodd RY. Blood donation screening for hepatitis B virus markers in the era of nucleic acid testing: are all tests of value? *Transfusion* 2012;52:440-6.
27. Kino S, Tomoda Y, Itoh Y, Karasaki H, Kasai S. Implementation of pre- and post-transfusion viral marker tests at Asahikawa medical college hospital. *Jpn J Transfus Cell Ther* 2009;55:21-8.
28. Hollinger FB, Dodd RY. Hepatitis B virus traceback and lookback: factors to consider. *Transfusion* 2009;49:176-84.
29. Yang MH, Li L, Hung YS, Hung CS, Allain JP, Lin KS, Tsai SJ. The efficacy of individual-donation and minipool testing to detect low-level hepatitis B virus DNA in Taiwan. *Transfusion* 2010;50:65-74.
30. Weber B, Melchior W, Gehrke R, Doerr HW, Berger A, Rabenau H. Hepatitis B virus markers in anti-HBc only positive individuals. *J Med Virol* 2001;64:312-9.
31. Bréchet C, Thiers V, Kremsdorf D, Nalpas B, Pol S, Paterlini-Bréchet P. Persistent hepatitis B virus infection in subjects without hepatitis B surface antigen: clinically significant or purely "occult"? *Hepatology* 2001;34:194-203.
32. Alhababi F, Sallam TA, Tong CY. The significance of "anti-HBc only" in the clinical virology laboratory. *J Clin Virol* 2003;27:162-9.
33. Levicnik-Stežinar S, Rahne-Potokar U, Candotti D, Lelie N, Allain JP. Anti-HBs positive occult hepatitis B virus carrier blood infectious in two transfusion recipients. *J Hepatol* 2008;48:1022-5.
34. Inaba S, Ito A, Miyata Y, Ishii H, Kajimoto S, Tanaka M, Maruta A, Saito S, Yugi H, Hino M, Tadokoro K. Individual nucleic amplification technology does not prevent all hepatitis B virus transmission by blood transfusion. *Transfusion* 2006;46:2028-9.
35. Candotti D, Allain JP. Transfusion-transmitted hepatitis B virus infection. *J Hepatol* 2009;51:798-809.
36. Liu CJ, Lo SC, Kao JH, Tseng PT, Lai MY, Ni YH, Yeh SH, Chen PJ, Chen DS. Transmission of occult hepatitis B virus by transfusion to adult and pediatric recipients in Taiwan. *J Hepatol* 2006;44:39-46. ■

Extensive gene deletions in Japanese patients with Diamond-Blackfan anemia

Madoka Kuramitsu,¹ Aiko Sato-Otsubo,² Tomohiro Morio,³ Masatoshi Takagi,³ Tsutomu Toki,⁴ Kiminori Terui,⁴ RuNan Wang,⁴ Hitoshi Kanno,⁵ Shouichi Ohga,⁶ Akira Ohara,⁷ Seiji Kojima,⁸ Toshiyuki Kitoh,⁹ Kumiko Goi,¹⁰ Kazuko Kudo,¹¹ Tadashi Matsubayashi,¹² Nobuo Mizue,¹³ Michio Ozeki,¹⁴ Atsuko Masumi,¹ Haruka Momose,¹ Kazuya Takizawa,¹ Takuo Mizukami,¹ Kazunari Yamaguchi,¹ Seishi Ogawa,² Etsuro Ito,⁴ and Isao Hamaguchi¹

¹Department of Safety Research on Blood and Biological Products, National Institute of Infectious Diseases, Tokyo, Japan; ²Cancer Genomics Project, Graduate School of Medicine, The University of Tokyo, Tokyo, Japan; ³Department of Pediatrics and Developmental Biology, Graduate School of Medicine, Tokyo Medical and Dental University, Bunkyo-ku, Tokyo, Japan; ⁴Department of Pediatrics, Hirosaki University Graduate School of Medicine, Hirosaki, Japan; ⁵Department of Transfusion Medicine and Cell Processing, Tokyo Women's Medical University, Tokyo, Japan; ⁶Department of Pediatrics, Graduate School of Medical Sciences, Kyushu University, Fukuoka, Japan; ⁷First Department of Pediatrics, Toho University School of Medicine, Tokyo, Japan; ⁸Department of Pediatrics, Nagoya University Graduate School of Medicine, Nagoya, Japan; ⁹Department of Hematology/Oncology, Shiga Medical Center for Children, Shiga, Japan; ¹⁰Department of Pediatrics, School of Medicine, University of Yamanashi, Yamanashi, Japan; ¹¹Division of Hematology and Oncology, Shizuoka Children's Hospital, Shizuoka, Japan; ¹²Department of Pediatrics, Seirei Hamamatsu General Hospital, Shizuoka, Japan; ¹³Department of Pediatrics, Kushiro City General Hospital, Hokkaido, Japan; and ¹⁴Department of Pediatrics, Graduate School of Medicine, Gifu University, Gifu, Japan

Fifty percent of Diamond-Blackfan anemia (DBA) patients possess mutations in genes coding for ribosomal proteins (RPs). To identify new mutations, we investigated large deletions in the RP genes *RPL5*, *RPL11*, *RPL35A*, *RPS7*, *RPS10*, *RPS17*, *RPS19*, *RPS24*, and *RPS26*. We developed an easy method based on quantitative-PCR in which the threshold cycle correlates to gene copy number. Using this approach, we were able to

diagnose 7 of 27 Japanese patients (25.9%) possessing mutations that were not detected by sequencing. Among these large deletions, similar results were obtained with 6 of 7 patients screened with a single nucleotide polymorphism array. We found an extensive intragenic deletion in *RPS19*, including exons 1-3. We also found 1 proband with an *RPL5* deletion, 1 patient with an *RPL35A* deletion, 3 with *RPS17* deletions, and 1 with an *RPS19*

deletion. In particular, the large deletions in the *RPL5* and *RPS17* alleles are novel. All patients with a large deletion had a growth retardation phenotype. Our data suggest that large deletions in RP genes comprise a sizable fraction of DBA patients in Japan. In addition, our novel approach may become a useful tool for screening gene copy numbers of known DBA genes. (*Blood*. 2012;119(10): 2376-2384)

Introduction

Diamond-Blackfan anemia (DBA; MIN# 105650) is a rare congenital anemia that belongs to the inherited BM failure syndromes, generally presenting in the first year of life. Patients typically present with a decreased number of erythroid progenitors in their BM.¹ A main feature of the disease is red cell aplasia, but approximately half of patients show growth retardation and congenital malformations in the craniofacial, upper limb, cardiac, and urinary systems. Predisposition to cancer, in particular acute myeloid leukemia and osteogenic sarcoma, is also characteristic of the disease.²

Mutations in the *RPS19* gene were first reported in 25% of DBA patients by Drapchinskaia et al in 1999.³ Since that initial finding, many genes that encode large (RPL) or small (RPS) ribosomal subunit proteins were found to be mutated in DBA patients, including *RPL5* (approximately 21%), *RPL11* (approximately 9.3%), *RPL35A* (3.5%), *RPS7* (1%), *RPS10* (6.4%), *RPS17* (1%), *RPS24* (2%), and *RPS26* (2.6%).⁴⁻⁷ To date, approximately half of the DBA patients analyzed have had a mutation in one of these genes. Konno et al screened 49 Japanese patients and found that 30% (12 of 49) carried mutations.⁸ In addition, our data showed that 22 of 68 DBA patients (32.4%) harbored a mutation in ribosomal protein (RP) genes (T.T., K.T., R.W., and E.I., unpub-

lished observation, April 16, 2011). These abnormalities of RP genes cause defects in ribosomal RNA processing, formation of either the large or small ribosome subunit, and decreased levels of polysome formation,^{4-6,9-12} which is thought to be one of the mechanisms for impairment of erythroid lineage differentiation.

Although sequence analyses of genes responsible for DBA are well established and have been used to identify new mutations, it is estimated that approximately half of the mutations remain to be determined. Because of the difficulty of investigating whole allele deletions, there have been few reports regarding allelic loss in DBA, and they have only been reported for *RPS19* and *RPL35A*.^{3,6,13} However, a certain percentage of DBA patients are thought to have a large deletion in RP genes. Therefore, a detailed analysis of allelic loss mutations should be conducted to determine other RP genes that might be responsible for DBA.

In the present study, we investigated large deletions using our novel approach for gene copy number variation analysis based on quantitative-PCR and a single nucleotide polymorphism (SNP) array. We screened Japanese DBA patients and found 7 patients with a large deletion in an allele in *RPL5*, *RPL35A*, *RPS17*, or *RPS19*. Interestingly, all of these patients with a large deletion had a phenotype of growth retardation, including short stature and

Submitted July 24, 2011; accepted November 15, 2011. Prepublished online as *Blood* First Edition paper, January 18, 2012; DOI 10.1182/blood-2011-07-368662.

The online version of this article contains a data supplement.

The publication costs of this article were defrayed in part by page charge payment. Therefore, and solely to indicate this fact, this article is hereby marked "advertisement" in accordance with 18 USC section 1734.

© 2012 by The American Society of Hematology

Table 1. Primers used for synchronized quantitative-PCR (s-q-PCR) of RPL proteins

Gene	Primer name	Sequence	Primer name	Sequence	Size, bp
RPL5	L5-02F	CTCCCAAAGTGCCTTGAGATTACAG	L5-02R	CACCTTTTCTCAACAAATTCCCAAT	132
	L5-05F	AGCCCTCCAACCTAGGTGACA	L5-05R	GAATTGGGATGGGCAAGAACT	102
	L5-17F	TGAACCCCTGCCCTAAACATG	L5-17R	TCTTGGTCAGGCCCTGCTTA	105
	L5-19F	ATTGTGCAAACTCGATCACTAGCT	L5-19R	GTGCTGAGGCTAACACATTTCAT	103
	L5-21F	GTGCCACTCTCTGGACAAACTG	L5-21R	CATAGGGCCAAAAGTCAAATAGAAG	102
	L5-28F	TCCACTTTAGGTAGCGAAACC	L5-28R	TCAGATTTGGCATGTACCTTTCA	102
RPL11	L11-06F	GCACCCACATGGCTTAAAGG	L11-6R	CAACCAACCCATAGGCCAAA	102
	L11-20F	GAGCCCCCTTTCTCAGATGATA	L11-20R	CATGAACCTGGGCTCTGAATCC	109
	L11-22F	TATGTGCAGATAAGAGGGCAGTCT	L11-22R	ATACAGATAAGGAACTGAGGCAGATT	98
RPL19	L19-02F	TGGCTCTCATAAAGGAAATCTCT	L19-02R	GGAATGCAGGCAAGTTACTCTGTT	103
	L19-08F	TTTGAAAGCAAGAAATAAGTTCCA	L19-08R	AGCACATCAGAGCTCCAAATAGG	107
	L19-16F	GGTTAGTTGAAGCAGGAGCCTTT	L19-16R	TGCTAGGGAGACAGAAAGCACATC	102
	L19-19F	GGACCAGTAGTTGTGACATCAGTTAAG	L19-19R	CCCATTGTAAACCCCACTTG	106
RPL26	L26-03F	TCAAAGAGCTGAGACAGAAGTACA	L26-03R	TCCATCAAGACAACGAGAACAAGT	102
	L26-16F	TTTGAGAATGCTTGAGAGAAAGGAA	L26-16R	TTCCAGCACATGTAATAATCAAGGA	102
	L26-18F	ATGTTTTATAAGCCCTCCAGTTGA	L26-18R	GAGAACAACAAGTTGAAAGGTTCA	102
	L26-20F	GGGCTTTGCTTGATCACTCTAGA	L26-20R	AGGGAGCCCGAAAACATTTAC	104
RPL35A	L35A-01F	TGTGGCTTCTATTTGCGTCAT	L35A-01R	GGAATTACCTCCTTTATTGCTACAAG	121
	L35A-07F	TTTCGGTTCTGTCTATTGCTGTGT	L35A-07R	GAACCCCTGAGTGGAGGATGTTT	113
	L35A-17F	GCCACAACTCCAGAGAATC	L35A-17R	GGATCACTTGAGGCCAGGAAT	104
	L35A-18F	TTAGGTGGGCTTTTCAGTCTCAA	L35A-18R	ATCTCCTGATTCACCACTTTGT	102
RPL36	L36-02F	CCGCTCTCAAGTGAAGAAATTTCTG	L36-02R	CTCCCTCTGCTGTGAAATGA	102
	L36-04F	TGCGTCTGCCAGGTGTTG	L36-04R	GGTAGCTGTGAGAACCAAGGT	105
	L36-17F	CCCCTGAAAGGACAGCAGTT	L36-17R	TTGGACACCAGGCACAGACT	114

Table 2. Primers used for s-q-PCR of RPS proteins

Gene	Primer name	Sequence	Primer name	Sequence	Size, bps
RPS7	S7-11F	GCGCTGCCAGATAGGAAATC	S7-11R	TTAGGGAGCTGCCTTACATATGG	102
	S7-12F	ACTGGCAGTTCTGTGATGCTAAGT	S7-12R	ACTCTTGCTCATCTCCAAAACCA	102
	S7-16F	GTGTCTGTGCCAGAAAGCTTGA	S7-16R	GAACCATGCAAAAGTGCCAATAT	112
RPS10	S10-03F	CTACGGTTTTGTGGGTCACTT	S10-03R	CATCTGCAAGAAGGAGACGATTG	102
	S10-15F	GTTGGCCTGGAGTCTGATTT	S10-15R	ATTCCAAGTGCACCAATTCCTT	101
	S10-17F	AATGGTGTTAGGCCAACGTTAC	S10-17R	TTTGAACAGTGGTTTTGTGCAT	100
RPS14	S14-03F	GAATTCAAAACCCCTTCTGCAA	S14-03R	TTGCTTCACTTACTCCTCAAGACATT	104
	S14-05F	ACAACAGCCCTCTACCTCTTTT	S14-05R	GGAAGACGCCGGCATTATT	102
	S14-06F	CGCCTCTACCTGCCAAC	S14-06R	GGGATCGGTGCTATTGTTATTC	102
	S14-09F	GCCATCATGCCGAAACATACT	S14-09R	AACGCCGACAGGAGAGA	102
	S14-13F	ATCAGGTGGAGCACAGGAAAC	S14-13R	GCGAGGGAGCTGCTTGATT	111
	S14-15F	AGAAGTTTTAGTGAGGCAGAAATGAGA	S14-15R	TCCCCTGGCTATTAATGAAACC	102
	S14-19F	GATGAATTGTCTTTCTCCATTCT	S14-19R	TAGCGGAAACCAAAAATGCT	102
RPS15	S15-11F	CTCAGTAAATAAGGCCGACATG	S15-11R	CCTCACACCAGCAACTGAAG	108
	S15-15F	GGTTGGAGAACATGGTGAAGTAACTA	S15-15R	CACATCCCTGGGCCACTCT	108
RPS17	S17-03F	ACTGCTGTGCTGGCTCGATT	S17-03R	GATGACCTGTCTTCTGGCCCTTA	121
	S17-05F	GAAAACAGATACAAATGGCATGGT	S17-05R	TGCCTCCACTTTTCCAGAGT	114
	S17-12F	CTATGTGTAGGAGGTCACAGATAG	S17-12R	CCACCTGGTACTGAGCACATGT	102
	S17-16F	TAGCGGAAGTTGTGTGCATTG	S17-16R	CAAGAACAGAAGCAGCCAGAG	102
	S17-18F	TGGCTGAATCTGCCTGCTT	S17-18R	GCCTTGTATGTACCTGGAATGG	103
	S17-20F	GGGCCCTTCCAAAATGTTGA	S17-20R	GCAAACTCTGTCCCTTTGAGAA	101
RPS19	S19-24F	CCATCCCAAGAATGCACACA	S19-24R	CGCCGTAGCTGGTACTCATG	120
	S19-28F	GACACACCTGTTGAGTCTCAGAGT	S19-28R	GCTTCTATTAAGTGAGCACACATCT	114
	S19-36F	CTCTTGAGGGTGGTCTGGAAT	S19-36R	GTCTTTGCGGGTTTCTCCTCTAC	102
	S19-40F	GGAACGGTGTGAGGATCAAG	S19-40R	AGCGGCTGTACACAGAAATG	101
	S19-44F	CTGAGGTTGAGTGTCCATTCT	S19-44R	GCACCGGCCTCTGTTATC	104
	S19-57F	CAGGGACACAGTGTGAGAAACT	S19-57R	TGAGATGTCCCATTTCACTATTGTT	101
	S19-58F	CATGATGTTAGCTCCGTTGCATA	S19-58R	ATTTTGGGAAGGTGAAGCTTAGGT	102
	S19-62F	GCAACAGAGCGAGACTCCATT	S19-62R	AGCACTTTTGGCCTACTTCTCA	102
RPS24	S19-65F	ACATTTCCAGAGCTGCATGA	S19-65R	TCGGACACCTAGACCTTGTCT	102
	S24-17F	CGACCAGCTGTGGCTTAGAGT	S24-17R	CCTTCATGCCAACCAAGTC	101
	S24-20F	ACAAGTAAGCATCATCACCTCGAA	S24-20R	TTTCCCTCACAGCTATCGTATGG	105
	S24-32F	GGGAAATGCTGTGCCACATACT	S24-32R	CTGTTTCATGGCTCCAGAGA	105
RPS26	S26-03F	CGCAGCAGTCAGGGACATT	S26-03R	AAGTTGGCGAAGGCTTTAAG	104
	S26-05F	ATGGAGGCCGTAGTTTGGT	S26-05R	TGCCTACCCTGAACCTTGTCT	102
RPS27A	S27A-09F	GCTGGAGTGCATTGCTTTGT	S27A-09R	CACGCCTGTAATCCCACTAA	102
	S27A-12F	CAGGCTTGGTGTGCTGTGACT	S27A-12R	ACGTCCATCTCCAGCTGCTT	103
	S27A-18F	GGGTTTTTCTGTTTGGTATTGTA	S27A-18R	AAAGGCGACTTTTGAAGTGT	111
	S27A-22F	TTACCATATTGCCAGTCTTCCATT	S27A-22R	TTCATATGCATTTGCACAACTGT	106

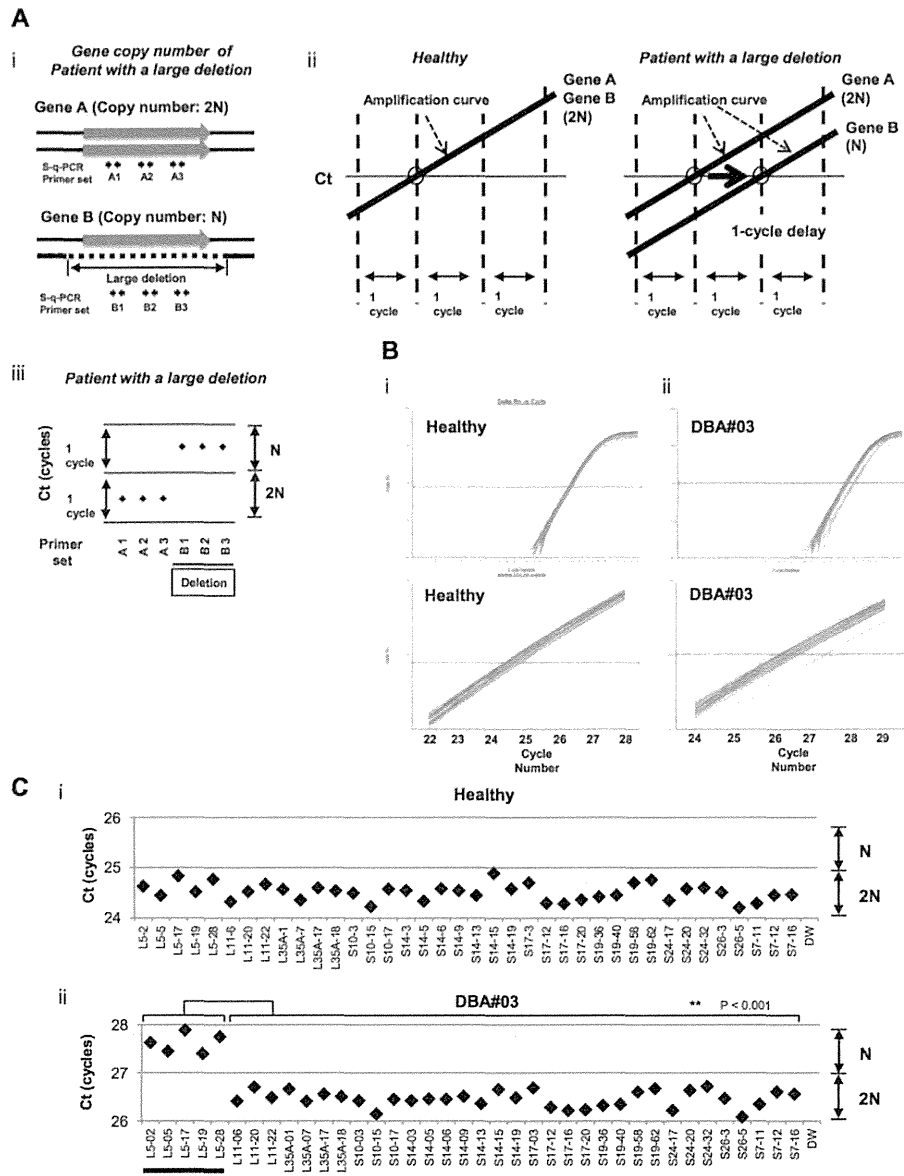


Figure 1. s-q-PCR can determine a large gene deletion in DBA. (A) Concept of the DBA s-q-PCR assay. The difference in gene copy number between a healthy sample and that with a large deletion is 2-fold (i). When all genomic s-q-PCR for genes of interest synchronously amplify DNA fragments, a 2-fold difference in the gene copy number is detected by a 1-cycle difference in the Ct scores of the s-q-PCR amplification curves (ii). Also shown is a dot plot of the Ct scores (iii). (B) Results of the amplification curves of s-q-PCR performed with a healthy person (i) and a DBA patient (patient 3; ii). The top panel shows the results of PCR cycles; the bottom panel is an extended graph of the PCR cycles at logarithmic amplification. (C) Graph showing Ct scores of s-q-PCR. If all specific primer sets for DBA genes show a 1-cycle delay relative to each other, this indicates a large deletion in the gene. Gene primer sets with a large deletion are underlined in the graph. ***P* < .001.

small-for-gestational age (SGA), which suggests that this is a characteristic of DBA patients with a large gene deletion in Japan.

tation of patients from a Japanese DBA genomic library are listed elsewhere or as reported by Konno et al.⁸ The study was approved by the institutional review board at the National Institute of Infectious Diseases and Hiroshima University.

Methods

Patient samples

Genomic DNA was extracted using the GenElute Blood Genomic DNA Kit (Sigma-Aldrich) according to the manufacturer's protocol. Clinical manifest-

DBA gene copy number assay by s-q-PCR

For s-q-PCR, primers were designed using Primer Express Version 3.0 software (Applied Biosystems). Primers are listed in Tables 1 and 2. Genomic DNA in water was denatured at 95°C for 5 minutes and

immediately cooled on ice. The composition of the s-q-PCR mixture was as follows: 5 ng of denatured genomic DNA, 0.4mM forward and reverse primers, 1× SYBR Premix Ex Taq II (Takara), and 1× ROX reference dye II (Takara) in a total volume of 20 μL (all experiments were performed in duplicate). Thermal cycling was performed using the Applied Biosystems 7500 fast real-time PCR system. Briefly, the PCR mixture was denatured at 95°C for 30 seconds, followed by 35 cycles of 95°C for 5 seconds, 60°C for 34 seconds, and then dissociation curve measurement. Threshold cycle (Ct) scores were determined as the average of duplicate samples. The technical errors of Ct scores in the triplicate analysis were within 0.2 cycles (supplemental Figure 1, available on the *Blood* Web site; see the Supplemental Materials link at the top of the online article). The sensitivity and specificity of this method was evaluated with 15 healthy samples. Any false positive was not observed in all primer sets in all healthy samples (supplemental Figure 2). We performed direct sequencing of the s-q-PCR products. The results of the sequence analysis were searched for using BLAST to confirm uniqueness. Sequence data were obtained from GenBank (<http://www.ncbi.nlm.nih.gov/genef/>) and Ensemble Genome Browser (<http://uswest.ensembl.org>).

Genomic PCR

Genomic PCR was performed using KOD FX (Toyobo) according to the manufacturer's step-down PCR protocol. Briefly, the PCR mixture contained 20 ng of genomic DNA, 0.4mM forward and reverse primers, 1mM dNTP, 1× KOD FX buffer, and 0.5 U KOD FX in a total volume of 25 μL in duplicate. Primers are given in supplemental Figure 3 and Table 2. PCR mixtures were denatured at 94°C for 2 minutes, followed by 4 cycles of 98°C for 10 seconds, 74°C for 12 minutes, followed by 4 cycles of 98°C for 10 seconds, 72°C for 12 minutes followed by 4 cycles of 98°C for 10 seconds, 70°C for 12 minutes, followed by 23 cycles of 98°C for 10 seconds and 68°C for 12 minutes. PCR products were loaded on 0.8% agarose gels and detected by LAS-3000 (Fujifilm).

DNA sequencing analysis

The genomic PCR product was purified by the GenElute PCR clean-up kit (Sigma-Aldrich) according to the manufacturer's instructions. Direct sequencing was performed using the BigDye Version 3 sequencing kit. Sequences were read and analyzed using a 3120x genetic analyzer (Applied Biosystems).

SNP array-based copy number analysis

SNP array experiments were performed according to the standard protocol of GeneChip Human Mapping 250K Nsp arrays (Affymetrix). Microarray data were analyzed for determination of the allelic-specific copy number using the CNAG program, as described previously.¹⁴ All microarray data are available at the EGA database (www.ebi.ac.uk/ega) under accession number EGAS00000000105.

Results

Construction of a convenient method for RP gene copy number analysis based on s-q-PCR

We focused on the heterozygous large deletions in DBA-responsible gene. The difference in copy number of genes between a mutated DBA allele and the intact allele was 2-fold (N and 2N; Figure 1Ai). If each PCR can synchronously amplify DNA fragments when the template genomic DNA used is of normal karyotype, it is possible to conveniently detect a gene deletion with a 1-cycle delay in s-q-PCR analysis (Figure 1Aii-iii).

Table 3. Summary of mutations and the mutation rate observed in Japanese DBA patients

Gene	Sequencing analysis
RPS19	10
RPL5	6
RPL11	3
RPS17	1
RPS10	1
RPS26	1
RPL35A	0
RPS24	0
RPS14	0
Mutations, n (%)	22 (32.4%)
Total analyzed, N	68

To apply this strategy for allelic analysis of DBA, we prepared primers for 16 target genes, *RPL5*, *RPL11*, *RPL35A*, *RPS10*, *RPS19*, *RPS26*, *RPS7*, *RPS17*, *RPS24*, *RPL9*, *RPL19*, *RPL26*, *RPL36*, *RPS14*, *RPS15*, and *RPS27A*, under conditions in which the Ct of s-q-PCR would occur within 1 cycle of that of the other primer sets (Tables 1 and 2). At the same time, we defined the criteria of a large deletion in our assay as follows. If multiple primer sets for one gene showed a 1-cycle delay from the other gene-specific primer set at the Ct score, we assumed that this represented a large deletion. As shown in Figure 1Bii and 1Cii, the specific primer sets for *RPL5* (L5-02, L5-05, L5-17, L5-19, and L5-28) detected a 1-cycle delay with respect to the mutated allele of patient 3. This assessment could be verified by simply confirming the difference of the cycles with the s-q-PCR amplification curves.

Study of large gene deletions in a Japanese DBA genomic DNA library

Sixty-eight Japanese DBA patients were registered and blood genomic DNA was collected at Hirosaki University. All samples were first screened for mutations in *RPL5*, *L11*, *L35A*, *S10*, *S14*, *S17*, *S19*, and *S26* by sequencing. Among these patients, 32.4% (22 of 68) had specific DBA mutations (Table 3 and data not shown). We then screened for large gene deletions in 27 patients from the remaining 46 patients who did not possess mutations as determined by sequencing (Table 4).

When we performed the s-q-PCR DBA gene copy number assay, 7 of 27 samples displayed a 1-cycle delay of Ct scores: 1 patient had *RPL5* (patient 14), 1 had *RPL35A* (patient 71), 3 had *RPS17* (patients 3, 60, 62), and 2 had *RPS19* (patients 24 and 72; Figure 2 and Table 4). Among these patients, the large deletions in the *RPL5* and *RPS17* genes are the first reported cases of allelic deletions in DBA. From these results, we estimate that a sizable number of Japanese DBA patients have a large deletion.

Based on our findings, the rate of large deletions was approximately 25.9% (7 of 27) in a category of unspecified gene mutations. Such mutations have typically gone undetected by conventional sequence analysis. We could not find any additional gene deletions in the analyzed samples.

Confirmation of the gene copy number for DBA genes by genome-wide SNP array

We performed genome-wide copy number analysis of the 27 DBA patients with a SNP array to confirm our s-q-PCR results. SNP array showed that patient 3 had a large deletion in

Table 4. Characteristics of DBA patients tested

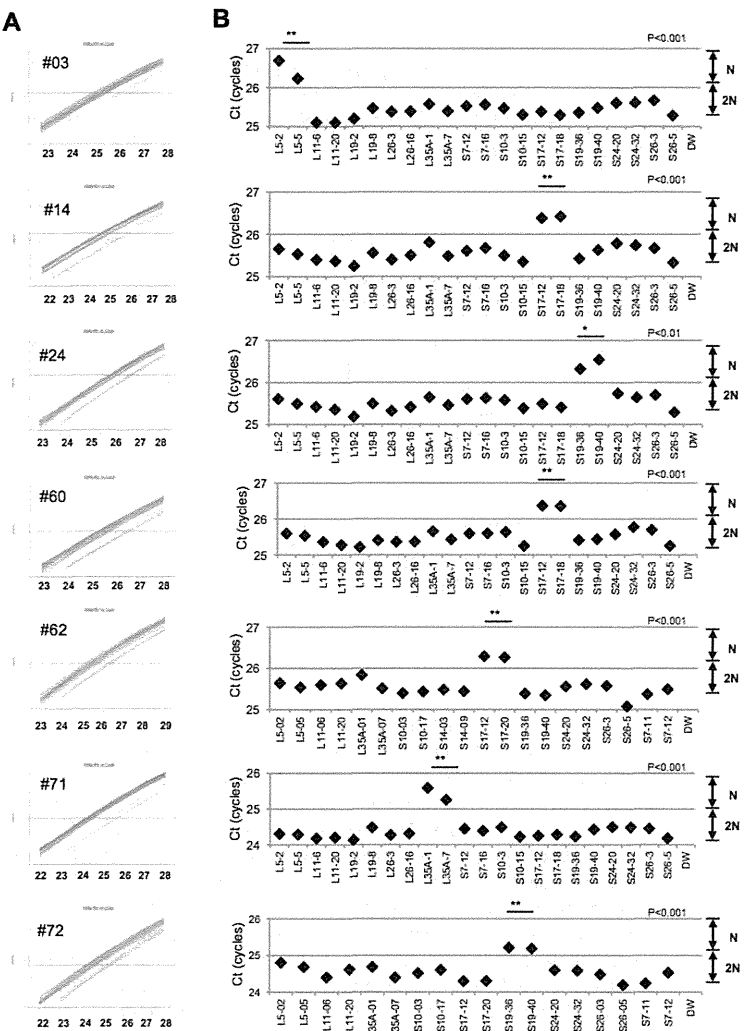
Patient no.	Age at diagnosis	Sex	Hb, g/dL	Large deletion by s-q-PCR	Large deletion by SNP array	Inheritance	Malformations	Response to first steroid therapy
Patients with a large deletion in RP genes								
3†	1 y	M		RPL5	RPL5	Sporadic	Short stature, thumb anomalies	Response
14*	5 y	M	5.5	RPS17	RPS17	Sporadic	White spots, short stature	Response
24*†	1 mo	F	5.5	RPS19	ND	Sporadic	Short stature, SGA	Response
60*†	2 mo	F	2.4	RPS17	RPS17	Sporadic	SGA	NT
62*†	1 mo	F	6.2	RPS17	RPS17	Sporadic	Small ASD, short stature, SGA	Response
71	0 y	M	5.3	RPL35A	RPL35A	Sporadic	Thumb anomalies, synostosis of radius and ulna, Cohelia Lange-like face, cleft palate, underdescended testis, short stature, cerebellar hypoplasia, fetal hydrops	NT
72†	0 y	M	2	RPS19	RPS19	Sporadic	Thumb anomalies, flat thenar, testicular hypoplasia, fetal hydrops, short stature, learning disability	No
Patients without a large deletion in RP genes								
5*	1 y	F	3.1	ND	ND	Sporadic	ND	Response
15*	1 mo	F	1.6	ND	ND	Sporadic	ND	Response
21*	1 y	F	2.6	ND	ND	Sporadic	ND	Response
26*	1 y 1 mo	F	8	ND	ND	Sporadic	Congenital hip dislocation, spastic quadriplegia, hypertelorism, nystagmus, short stature, learning disability	Response
33*	2 mo	F	1.3	ND	ND	Sporadic	ND	Response
36*	0 y	M	8.2	ND	ND	Familial	ND	Response
37*	4 y	M	6.1	ND	ND	Sporadic	Hypospadias, underdescended testis, SGA	NT
45*	5 d	M	5.1	ND	ND	Sporadic	Short stature, microcephaly, mental retardation, hypogammaglobulinemia	Poor
50*	2 m	F	3.4	ND	ND	Familial	ND	Response
61*	9 m	M	4	ND	ND	Sporadic	ND	Response
63*	0 y	M	6.8	ND	ND	Sporadic	Micrognathia, hypertelorism, short stature	Response
68	1 y 4 mo	M	5.9	ND	ND	Sporadic	ND	NT (CR)
69	1 y	M	9.3	ND	ND	Sporadic	ND	Response
76	0 y	M	4	ND	ND	Sporadic	ND	Response
77	0 y	M	7.8	ND	ND	Familial	Short stature	No
83	9 mo	F	3	ND	ND	Sporadic	ND	NT
90	10 mo	M	9	ND	ND	Sporadic	ND	No
91	0 y	F	3.8	ND	ND	Sporadic	ND	Response
92	2 mo	M	3.7	ND	ND	Sporadic	ASD, PFO, melanosis, underdescended testis, SGA, short stature	Response
93	11 mo	M	2.2	ND	ND	Sporadic	White spots, senile face, corneal opacity, underdescended testis, syndactyly, ectrodactyly, flexion contracture, extension contracture	Response

ND indicates not detected; NT, not tested; CR, complete remission; ASD, atrial septal defect; and PFO, persistent foramen ovale.

*Status data of Japanese probands 3 to 63 is from a report by Konno et al.⁹

†Large deletions of the parents of 5 DBA patients (3, 24, 60, 62, and 72) were analyzed by s-q-PCR, but there were no deletions in DBA genes in any of the 5 pairs of parents.

Figure 2. Detection of 7 mutations with a large deletion in DBA patients. Genomic DNA of 27 Japanese DBA patients with unknown mutations were subjected to the DBA gene copy number assay. (A) Amplification curve of s-q-PCR of a mutation with a large deletion. The deleted gene can be easily distinguished. (B) Ct score (cycles) of representative s-q-PCR with DBA genomic s-q-PCR primers. Results of the 2 gene-specific primer pairs indicated in the graph are representative of at least 2 sets for each gene-specific primer (carried out in the same run). ** $P < .001$; * $P < .01$



chromosome 1 (ch1) spanning 858 kb (Figure 3A); patient 71 had a large deletion in ch3 spanning 786 kb (Figure 3B); patients 14, 60, and 62 had a large deletion in ch15 spanning 270 kb, 260 kb, and 330 kb, respectively (Figure 3C); and patient 72 had a large deletion in ch19 spanning 824 kb (Figure 3D). However, there were no deletions detected in ch19 in patient 24 (Figure 3D). Genes estimated to reside within a large deletion are listed in supplemental Table 1. Consistent with these s-q-PCR results, 6 of 7 large deletions were detected and confirmed as deleted regions, and these large deletions contained *RPL5*, *RPL35A*, *RPS17*, and *RPS19* (Table 4 and supplemental Table 1). Other large deletions in RP genes were not detected by this analysis. From these results, we conclude that the synchronized multiple PCR amplification method has a detection sensitivity comparable to that of SNP arrays.

Detailed examination of a patient with intragenic deletion in the *RPS19* allele (patient 24)

Interestingly, for patient 24, in whom we could not detect a large deletion by SNP array at s-q-PCR gene copy number analysis, 2 primer sets for *RPS19* showed a 1-cycle delay (*RPS19-36* and *RPS19-40*), but 2 other primer pairs (*RPS19-58* and *RPS19-62*) did not show this delay (Figure 4A). We attempted to determine the deleted region in detail by testing more primer sets on *RPS19*. We tested a total of 9 primer sets for *RPS19* (Figure 4B) and examined the gene copy numbers. Surprisingly, 4 primer sets (*S19-24*, *S19-36*, *S19-40*, and *S19-44*) for intron 3 of *RPS19* indicated a 1-cycle delay, but the other primers for *RPS19* located on the 5' untranslated region (5'UTR), intron 3, or 3'UTR did not show this delay (*S19-57*, *S19-58*, *S19-28*, *S19-62*, and *S19-65*; Figure 4B-C). These results suggest that the intragenic deletion occurred in the *RPS19* allele. To confirm this deleted region precisely, we performed genomic PCR on *RPS19*, amplifying a region from the 5'UTR to intron 3 (Figure

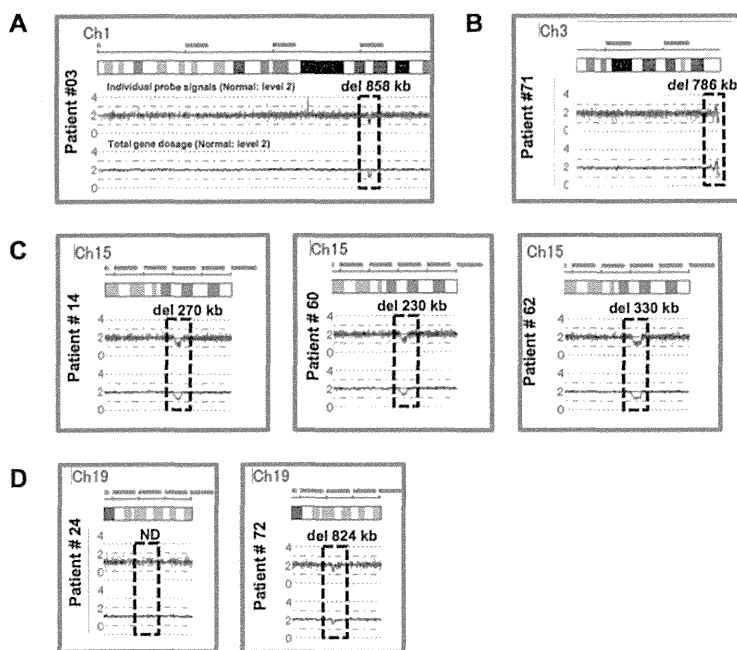


Figure 3. Results of SNP genomic microarray (SNP-chip) analysis. Genomic DNA of 27 Japanese DBA patients with unknown mutations was examined using a SNP array. Six patients had large deletions in their chromosome (ch), which included one DBA-responsible gene. Patient 3 has a large deletion in ch1 (A), patient 71 has a deletion in ch3 (B), patients 14, 60, and 62 have deletions in ch15 (C), and patient 72 has a deletion in ch19 (D).

4B). In patient 24, we observed an abnormally sized PCR product at a low molecular weight by agarose gel electrophoresis (Figure 4D). We did not detect a wild-type PCR product from the genomic PCR. This finding is probably because PCR tends to amplify smaller molecules more easily. However, we did detect a PCR fragment at the correct size using primers located in the supposedly deleted region. These bands were thought to be from the products of a wild-type allele. Sequencing of the mutant band revealed that intragenic recombination occurred at a homologous region of 27 nucleotides, from -1400 to -1374 in the 5' region, to $+5758$ and $+5784$ in intron 3, which resulted in the loss of 7157 base pairs in the *RPS19* gene (Figure 4E). The deleted region contains exons 1, 2, and 3, and therefore the correct *RPS19* mRNA could not be transcribed.

Genotype-phenotype analysis and DBA mutations in Japan

Patients with a large deletion in DBA genes had common phenotypes (Table 4). Malformation with growth retardation (GR), including short stature or SGA, were observed in all 7 patients. In patients who had a mutation found by sequencing, half had GR (11 of 22; status data of DBA patients with mutations found by sequencing are not shown). GR may be a distinct phenotypic feature of large deletion mutations in Japanese DBA patients. Familial mutations were analyzed for parents for 5 DBA patients with a large deletion (patients 3, 24, 60, 62, and 72) by s-q-PCR. There are no large deletions in all 5 pairs of parents in DBA-responsible genes. Four of the 7 patients responded to steroid therapy. We have not observed significant phenotypic differences between patients with extensive deletions and other patients with regard to blood counts, responsiveness to treatment, or other malformations.

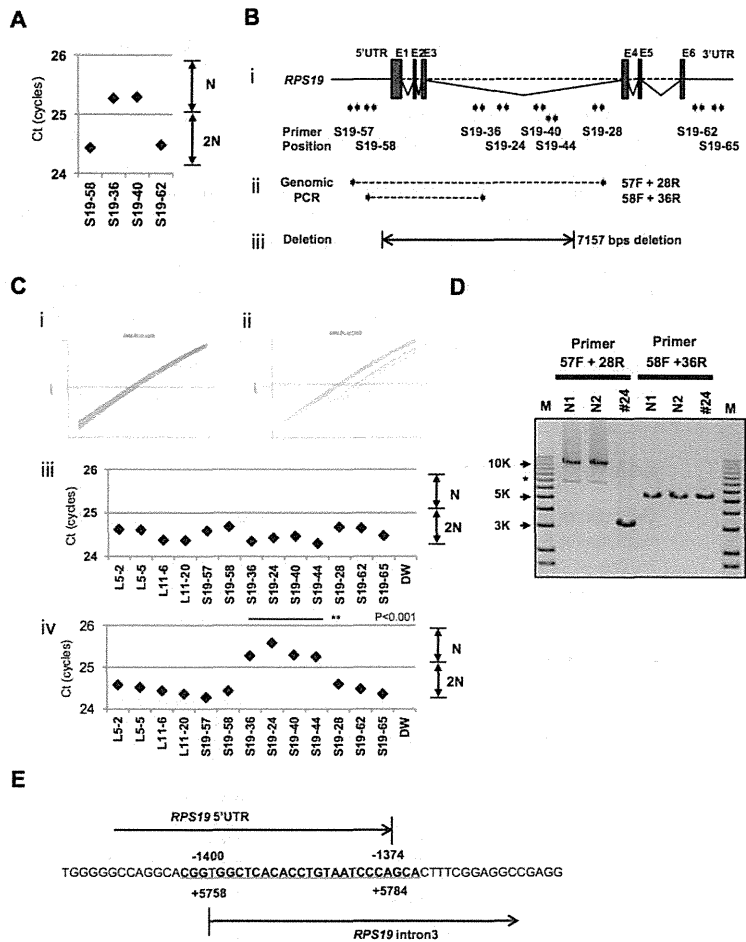
Discussion

Many studies have reported RP genes to be responsible for DBA. However, mutations have not been determined for approximately half of DBA patients analyzed. There are 2 possible reasons for this finding. One possibility is that patients have other genes responsible for DBA, and the other is that patients have a complicated set of mutations in RP genes that are difficult to detect. In the present study, we focused on the latter possibility because we have found fewer Japanese DBA patients with RP gene mutations (32.4%) compared with another cohort study of 117 DBA patients and 9 RP genes (approximately 52.9%).⁴ With our newly developed method, we identified 7 new mutations with a large deletion in *RPL5*, *RPL35A*, *RPS17*, and *RPS19*.

The frequency of a large deletion was approximately 25.9% (7 of 27) in our group of patients who were not found to have mutations by genomic sequencing. Therefore, total RP gene mutations were confirmed in 42.6% of these Japanese patients (Table 5). Interestingly, mutations in *RPS17* have been observed at a high rate (5.9%) in Japan relative to that in other countries (1%).^{5,15,16} Although the percentage of DBA mutations differs among different ethnic groups,^{8,17-19} a certain portion of large deletions in DBA-responsible genes are likely to be determined in other countries by new strategies.

In the present study, we analyzed patient data to determine genotype-phenotype relations. To date, large deletions have been reported with *RPS19* and *RPL35A* in DBA patients.^{3,6,13} *RPS19* large deletions/translocations have been reported in 12 patients, and *RPL35A* large deletions have been reported in 2 patients.¹⁹ GR in patients with a large deletion has been observed previously with *RPS19* translocations,^{3,19-21} but it was not found in 2 patients with *RPL35A* deletion.⁶ Interestingly, all of our patients with a large deletion had a phenotype

Figure 4. Result of s-q-PCR gene copy number assay for patient 24. (A) Results of s-q-PCR gene copy number assay for *RPS19* with 4 primer sets. (B) The *RPS19* gene copy number was analyzed with 9 specific primer sets for *RPS19* that span from the 5'UTR to the 3'UTR. (ii) Primer positions of genomic PCR for *RPS19*. (iii) Region determined to be an intragenic deletion in *RPS19*. (C) Results of gene copy number assay for *RPS19* show a healthy person (i,iii) and a DBA patient (ii,iv), and Ct results are shown (iii-iv). Patient 24 showed a "1-cycle delay" with primers located in the intron 3 region, but other primer sets were normal. (D) Results of genomic PCR amplification visualized by agarose gel electrophoresis to determine the region of deletion. N1 and N2 are healthy samples. *Nonspecific band. (E) Results from the genomic sequence of the 3-kb DNA band from genomic PCR on patient 24 showing an intragenic recombination from -1400 to 5784 (7157 nt) in *RPS19*. ** $P < .001$.



of GR, including short stature and SGA, which suggests that this is a characteristic of DBA with a large gene deletion in Japan. Our study results suggest the possibility that GR is associated with extensive deletion in Japanese patients. Although further case studies will be needed to confirm this possibility, screening of DBA samples using our newly developed method will help to advance our understanding of the broader implications of the mutations and the correlation with the DBA genotype-phenotype.

Table 5. Total mutations in Japanese DBA patients, including large gene deletions

Gene	Mutation rate
RPS19	12(17.6%)
RPL5	7(10.3%)
RPL11	3 (4.4%)
RPS17	4 (5.9%)
RPS10	1 (1.5%)
RPS26	1 (1.5%)
RPL35A	1 (1.5%)
RPS24	0
RPS14	0
Mutations, n (%)	29(42.6%)
Total analyzed, N	68

Copy number variation analysis of DBA has been performed by linkage analysis, and the *RPS19* gene was first identified as a DBA-susceptibility gene. Comparative genomic hybridization array technology has also been used to detect DBA mutations in *RPL35A*, and multiplex ligation-dependent probe amplification has been used for *RPS19* gene deletion analysis.^{3,6,13,22} However, these analyzing systems have problems in mutation screening. Linkage analysis is not a convenient tool to screen for multiple genetic mutations, such as those in DBA, because it requires a high level of proficiency. Although comparative genomic hybridization technology is a powerful tool with which to analyze copy number comprehensively, this method requires highly specialized equipment and analyzing software, which limits accessibility for researchers. Whereas quantitative PCR-based methods for copy number variation analysis are commercially available (TaqMan), they require a standard curve for each primer set, which limits the number of genes that can be loaded on a PCR plate. To address this issue, a new method of analysis is needed. By stringent selection of PCR primers, the s-q-PCR method enables analysis of many DBA genes in 1 PCR plate and the ability to immediately distinguish a large deletion using the s-q-PCR amplification curve. In our study, 6 of 7 large deletions in the RP gene detected by s-q-PCR were confirmed by SNP arrays (Figure 3). Interestingly, we detected

1 large intragenic deletion in *RPS19*, which was not detected by the SNP array. This agreement between detection results suggests that the s-q-PCR copy number assay could be useful for detecting large RP gene deletions.

In the present study, 7 DBA patients carried a large deletion in the RP genes. This type of mutation could be underrepresented by sequencing analysis, although in the future, genome sequencing might provide a universal platform for mutation and deletion detection. We propose that gene copy number analysis for known DBA genes, in addition to direct sequencing, should be performed to search for a novel responsible gene for DBA. Although at present, it may be difficult to observe copy numbers on all 80 ribosomal protein genes in one s-q-PCR assay, our method allows execution of gene copy number assays for several target genes in 1 plate. Because our method is quick, easy, and low cost, it could become a conventional tool for detecting DBA mutations.

Acknowledgments

The authors thank Momoka Tsuruhara, Kumiko Araki, and Keiko Furuhashi for their expert assistance.

This work was partially supported by grants-in-aid for scientific research from the Ministry of Education, Culture, Sports, Science and Technology of Japan, and by Health and Labor Sciences

research grants (Research on Intractable Diseases) from the Ministry of Health, Labor and Welfare of Japan.

Authorship

Contribution: M.K. designed and performed the research, analyzed the data, and wrote the manuscript; A.S.-O. and S. Ogawa performed the SNP array analysis; T.M., M.T., and M.O. designed the study; T.T., K. Terui, and R.W. analyzed the mutations and status data; H.K., S. Ohga, A.O., S.K., T.K., K.G., K.K., T.M., and N.M. analyzed the status data; A.M., H.M., K. Takizawa, T.M., and K.Y., performed the research and analyzed the data; E.I. and I.H. designed the study and analyzed the data; and all authors wrote the manuscript.

Conflict-of-interest disclosure: The authors declare no competing financial interests.

Correspondence: Isao Hamaguchi, MD, PhD, Department of Safety Research on Blood and Biological Products, National Institute of Infectious Diseases, 4-7-1, Gakuen, Musashimurayama, Tokyo 208-0011, Japan; e-mail: 130hama@nih.go.jp; or Etsuro Ito, MD, PhD, Department of Pediatrics, Hirosaki University Graduate School of Medicine, 5 Zaifucho, Hirosaki, Aomori 036-8562, Japan; e-mail: eturou@cc.hirosaki-u.ac.jp.

References

1. Hamaguchi I, Flygare J, Nishiura H, et al. Proliferation deficiency of multipotent hematopoietic progenitors in ribosomal protein S19 (*RPS19*)-deficient diamond-Blackfan anemia improves following *RPS19* gene transfer. *Mol Ther*. 2003;7(5 pt 1):613-622.
2. Vlachos A, Ball S, Dahl N, et al. Diagnosing and treating Diamond-Blackfan anaemia: results of an international clinical consensus conference. *Br J Haematol*. 2008;142(6):859-876.
3. Drachtchinskaja N, Gustavsson P, Andersson B, et al. The gene encoding ribosomal protein S19 is mutated in Diamond-Blackfan anaemia. *Nat Genet*. 1999;21(2):169-175.
4. Doherty L, Sheen MR, Vlachos A, et al. Ribosomal protein genes *RPS10* and *RPS26* are commonly mutated in Diamond-Blackfan anemia. *Am J Hum Genet*. 2010;86(2):222-228.
5. Gazda HT, Sheen MR, Vlachos A, et al. Ribosomal protein L5 and L11 mutations are associated with cleft palate and abnormal thumbs in Diamond-Blackfan anemia patients. *Am J Hum Genet*. 2008;83(6):769-780.
6. Farrar JE, Nater M, Caywood E, et al. Abnormalities of the large ribosomal subunit protein, Rpl35a, in Diamond-Blackfan anemia. *Blood*. 2008;112(5):1582-1592.
7. Gazda HT, Grabowska A, Merida-Long LB, et al. Ribosomal protein S24 gene is mutated in Diamond-Blackfan anemia. *Am J Hum Genet*. 2006;79(6):1110-1118.
8. Konno Y, Toki T, Tandai S, et al. Mutations in the ribosomal protein genes in Japanese patients with Diamond-Blackfan anemia. *Haematologica*. 2010;95(8):1293-1299.
9. Robledo S, Idol RA, Crimmins DL, Ladenson JH, Mason PJ, Bessler M. The role of human ribosomal proteins in the maturation of rRNA and ribosome production. *RNA*. 2008;14(9):1918-1929.
10. Léger-Silvestre I, Caffrey JM, Dawallby R, et al. Specific Role for Yeast Homologs of the Diamond-Blackfan Anemia-associated Rps19 Protein in Ribosome Synthesis. *J Biol Chem*. 2005;280(46):38177-38185.
11. Choessel V, Fribourg S, Aguisa-Toure AH, et al. Mutation of ribosomal protein RPS24 in Diamond-Blackfan anemia results in a ribosome biogenesis disorder. *Hum Mol Genet*. 2008;17(9):1253-1263.
12. Flygare J, Aspesi A, Bailey JC, et al. Human RPS19, the gene mutated in Diamond-Blackfan anemia, encodes a ribosomal protein required for the maturation of 40S ribosomal subunits. *Blood*. 2007;109(3):980-986.
13. Quarello P, Garelli E, Brusco A, et al. Multiplex ligation-dependent probe amplification enhances molecular diagnosis of Diamond-Blackfan anemia due to *RPS19* deficiency. *Haematologica*. 2008;93(11):1748-1750.
14. Yamamoto G, Nannya Y, Kato M, et al. Highly sensitive method for genomewide detection of allelic composition in nonpaired, primary tumor specimens by use of affymetrix single-nucleotide-polymorphism genotyping microarrays. *Am J Hum Genet*. 2007;81(1):114-126.
15. Song MJ, Yoo EH, Lee KO, et al. A novel initiation codon mutation in the ribosomal protein S17 gene (*RPS17*) in a patient with Diamond-Blackfan anemia. *Pediatr Blood Cancer*. 2010;54(4):629-631.
16. Cmejla R, Cmejlova J, Handrkova H, Petrak J, Pospisilova D. Ribosomal protein S17 gene (*RPS17*) is mutated in Diamond-Blackfan anemia. *Hum Mutat*. 2007;28(12):1178-1182.
17. Cmejla R, Cmejlova J, Handrkova H, et al. Identification of mutations in the ribosomal protein L5 (*RPL5*) and ribosomal protein L11 (*RPL11*) genes in Czech patients with Diamond-Blackfan anemia. *Hum Mutat*. 2009;30(3):321-327.
18. Quarello P, Garelli E, Carando A, et al. Diamond-Blackfan anemia: genotype-phenotype correlations in Italian patients with *RPL5* and *RPL11* mutations. *Haematologica*. 2010;95(2):206-213.
19. Boria I, Garelli E, Gazda HT, et al. The ribosomal basis of Diamond-Blackfan Anemia: mutation and database update. *Hum Mutat*. 2010;31(12):1269-1279.
20. Campagnoli MF, Garelli E, Quarello P, et al. Molecular basis of Diamond-Blackfan anemia: new findings from the Italian registry and a review of the literature. *Haematologica*. 2004;89(4):480-489.
21. Willig TN, Drachtchinskaja N, Dianzani I, et al. Mutations in ribosomal protein S19 gene and diamond blackfan anemia: wide variations in phenotypic expression. *Blood*. 1999;94(12):4294-4306.
22. Gustavsson P, Garelli E, Drachtchinskaja N, et al. Identification of microdeletions spanning the Diamond-Blackfan anemia locus on 19q13 and evidence for genetic heterogeneity. *Am J Hum Genet*. 1998;63(5):1388-1395.

The earliest thymic T cell progenitors sustain B cell and myeloid lineage potential

Sidinh Luc¹⁻³, Tiago C Luis^{1,10}, Hanane Boukarabila^{1,10}, Iain C Macaulay¹, Natalija Buza-Vidas^{1,4}, Tiphaine Bouriez-Jones¹, Michael Lutteropp^{1,3}, Petter S Woll¹, Stephen J Loughran¹, Adam J Mead¹, Anne Hultquist², John Brown³, Takuo Mizukami¹, Sahoko Matsuoka¹, Helen Ferry^{1,9}, Kristina Anderson², Sara Duarte¹, Deborah Atkinson¹, Shamit Soneji³, Aniela Domanski¹, Alison Farley⁴, Alejandra Sanjuan-Pla⁴, Cintia Carella⁵, Roger Patient³, Marella de Bruijn³, Tariq Enver^{3,9}, Claus Nerlov⁴, Clare Blackburn⁴, Isabelle Godin⁶⁻⁸ & Sten Eirik W Jacobsen¹⁻³

The stepwise commitment from hematopoietic stem cells in the bone marrow to T lymphocyte-restricted progenitors in the thymus represents a paradigm for understanding the requirement for distinct extrinsic cues during different stages of lineage restriction from multipotent to lineage-restricted progenitors. However, the commitment stage at which progenitors migrate from the bone marrow to the thymus remains unclear. Here we provide functional and molecular evidence at the single-cell level that the earliest progenitors in the neonatal thymus had combined granulocyte-monocyte, T lymphocyte and B lymphocyte lineage potential but not megakaryocyte-erythroid lineage potential. These potentials were identical to those of candidate thymus-seeding progenitors in the bone marrow, which were closely related at the molecular level. Our findings establish the distinct lineage-restriction stage at which the T cell lineage-commitment process transits from the bone marrow to the remote thymus.

At the heart of developmental and stem-cell biology, as well as regenerative medicine, is the fundamental process of lineage commitment from self-renewing multipotent stem cells to lineage-restricted progenitors. In all species and organ systems, this process occurs first during embryonic development but is recapitulated postnatally and in adult life by adult multipotent stem cells that replenish cell lineages with a limited lifespan. Hematopoiesis represents the mammalian paradigm of how multilineage diversity can be achieved through the commitment of multipotent stem cells to lineage-committed progenitors and the establishment of distinct blood cell lineages¹. However, the exact cellular commitment pathways remain unclear^{1,2}.

Whereas lineage-restricted progenitors for all other blood cell lineages can be generated from self-renewing hematopoietic stem cells (HSCs) in the postnatal bone marrow, the final steps of restriction to the T lymphocyte lineage take place in the thymus³. Because the thymus cannot sustain HSCs, continuous thymopoiesis can be secured only through regular replenishment by bone marrow-resident thymus-seeding progenitors (TSPs)⁴. However, the commitment stage(s) at which these progenitors migrate from the bone marrow to the thymus is (are) unknown. The thymus contains multiple blood cell lineages^{5,6}, as does the bone marrow; however, the identification

of multipotent progenitors in the thymus that match the lineage potential of candidate TSPs in the bone marrow has not been possible so far. Early thymic progenitors (ETPs) have been extensively studied in the adult thymus, but their exact lineage potentials and relationship to candidate TSPs in the bone marrow have remained unclear⁷.

Studies evaluating the lineage potential of ETPs at the single-cell level have shown that a large fraction of ETPs from adult mice have combined T cell and myeloid (granulocyte-monocyte (GM)) potential^{8,9}. B cell lineage potential, however, was not detected for single, highly purified ETPs from adult mice, which suggests that the most primitive progenitor in the thymus might have potential restricted to T cells and granulocytes-monocytes^{8,9}. Similar studies of fetal thymus have supported the proposal that the potential of ETPs is restricted to T cells and granulocytes-monocytes and have failed to show any B cell potential^{10,11}. However, other studies have reported even rarer ETPs from adult mice with combined T cell and B cell (but not myeloid) potential⁶, and candidate TSPs identified in the bone marrow⁷, such as common lymphoid progenitors (CLPs)¹², lymphoid-primed multipotent progenitors (LMPPs)¹³ and HSCs¹, all have B cell potential. The megakaryocyte-erythroid (MkE) potential of ETPs is of particular relevance to the ongoing debate on whether

¹Haematopoietic Stem Cell Laboratory, Weatherall Institute of Molecular Medicine, John Radcliffe Hospital, University of Oxford, Oxford, UK. ²Hematopoietic Stem Cell Laboratory, Lund Stem Cell Center, Lund University, Lund, Sweden. ³Medical Research Council Molecular Haematology Unit, Weatherall Institute of Molecular Medicine, University of Oxford, Oxford, UK. ⁴Institute for Stem Cell Research, Medical Research Council Centre for Regenerative Medicine, University of Edinburgh, Edinburgh, UK. ⁵European Molecular Biology Laboratory Mouse Biology Unit, Monterotondo, Italy. ⁶Institut National de la Santé et de la Recherche Médicale U1009, Villejuif, France. ⁷Institut Gustave Roussy, Villejuif, France. ⁸University of Paris-Sud, Orsay, France. ⁹Present addresses: Experimental Medicine Division, Nuffield Department of Clinical Medicine, John Radcliffe Hospital, Oxford, UK (H.F.) and University College London Cancer Institute, London, UK (T.E.). ¹⁰These authors contributed equally to this work. Correspondence should be addressed to S.E.W.J. (sten.jacobsen@imm.ox.ac.uk).

Received 1 August 2011; accepted 1 February 2012; published online 19 February 2012; doi:10.1038/ni.2255



the first lineage-commitment step in hematopoiesis results in strict separation into common pathways for commitment to the myeloid and lymphoid lineage, as presented in the still-prevailing textbook hierarchical model of hematopoiesis^{1,14}, or whether early lymphoid progenitors sustain GM potential but not Mke potential^{2,13,15}, as reported in human studies as well^{16,17}. The Mke potential of purified ETPs has yet to be investigated^{5,6,8,9}.

The fact that no multipotent thymic progenitors with the same lineage potentials as those of candidate multipotent TSPs in the bone marrow have been identified yet contributes to the considerable gap in understanding of the distinct roles of the local bone marrow and thymus environments in promoting distinct prethymic and thymic stages of commitment to the T cell lineage. Here we demonstrate at

the single-cell level the existence of postnatal ETPs with combined T cell, GM and B cell potential but no Mke potential, establishing the exact lineage commitment step at which the multipotent T lymphocyte progenitors must migrate to the thymus to allow the final steps of restriction to the T cell lineage to be completed. The data reported here provide further support for a myeloid-based model of commitment of hematopoietic-lineage cells to the T cell lineage.

RESULTS

ETPs have combined T cell, B cell and GM potential

The present knowledge about candidate TSPs and ETPs can be reconciled (Supplementary Fig. 1) only if a progenitor restricted to the T cell-GM lineage can be identified in the bone marrow, a T cell-GM

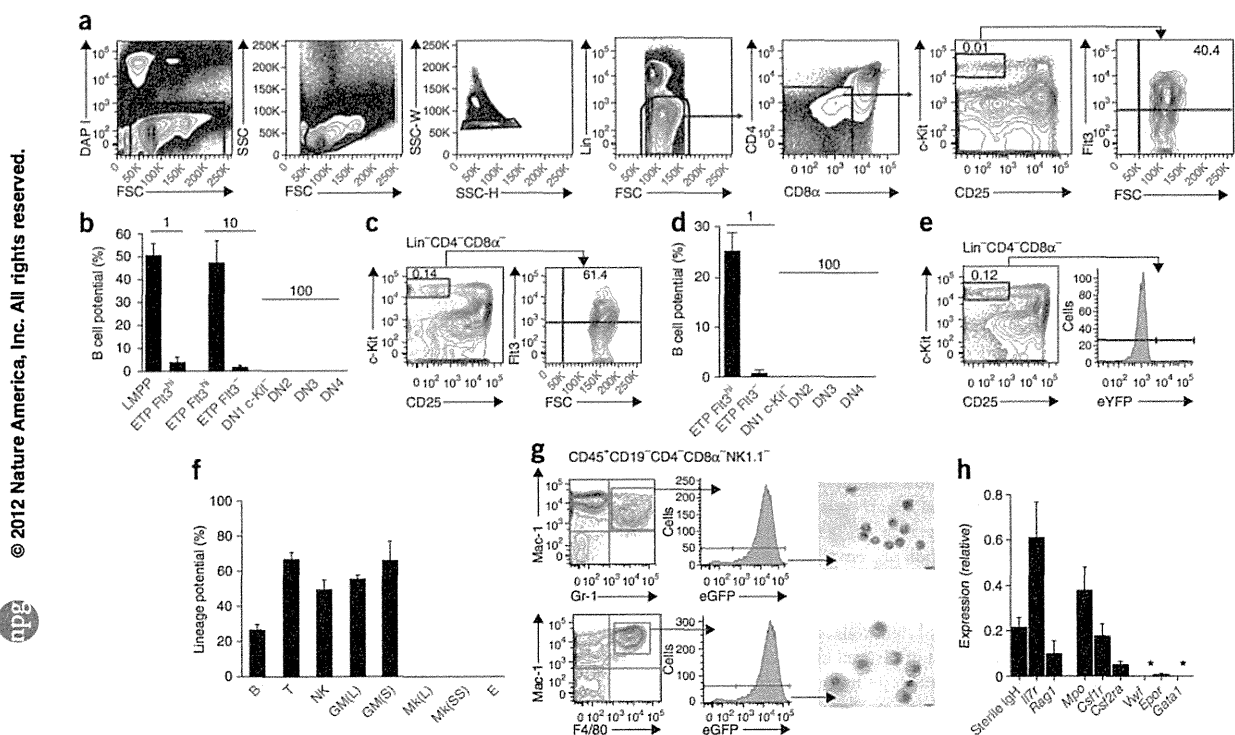


Figure 1 ETPs are multipotent lympho-myeloid restricted progenitors. (a) Flow cytometry profiles and gating strategies for the detection of Lin⁻CD4⁻CD8 α ⁻CD25⁻c-Kit^{hi}Flt3^{hi} ETPs from young adult mice (4–6 weeks). Numbers in plots indicate percent ETPs among total thymocytes. DAPI, DNA-intercalating dye; FSC, forward scatter; SSC, side scatter; -W, width; -H, height. (b) Frequency of B cell potential of cultures seeded with a single Lin⁻Sca-1⁺c-Kit⁺Flt3^{hi} bone marrow cell (LMPP; $n = 320$); a single Flt3^{hi} ETP ($n = 73$ cells) or ten Flt3^{hi} ETPs ($n = 960$ cells); ten Flt3⁻ ETPs ($n = 960$ cells); or other DN thymocyte progenitor populations (DN1–DN4; $n = 2,400$ cells (seeded with 100 cells per well)), all from adult mice. (c) Flow cytometry profiles and gating strategies as in a, for cells from newborn mice (1 d). (d) Frequency of B cell potential as in b, for cultures of cells from newborn mice, seeded as single Flt3^{hi} ETPs ($n = 348$ cells) or single Flt3⁻ ETPs ($n = 210$ cells), and other DN thymocyte progenitor populations seeded at 100 cells per culture ($n = 4,200$ – $6,000$ cells). (e) Expression of enhanced yellow fluorescent protein (eYFP) in ETPs from neonatal mice ($n = 4$) expressing Cre from the *Cd79a* promoter. (f) Frequency of cells with B cell potential (B; $n = 348$ cells), T cell potential (T; $n = 204$ cells), natural killer cell potential (NK; $n = 48$ cells), GM potential (grown in liquid (GM(L); $n = 600$ cells) or on stroma (GM(S); $n = 64$ cells)), megakaryocyte potential (grown in liquid (Mk(L); $n = 1,080$ cells) or on semisolid support (Mk(SS); $n = 6$; 200 cells per replicate)) or erythroid potential (E; $n = 8$; 500–1,000 cells per replicate) among Flt3⁺ ETPs from neonatal mice (positive controls, Supplementary Fig. 5). (g) Expression of myeloid markers Mac-1 and lysozyme M (reported as eGFP expression; left and middle), and morphological analysis (right) of sorted granulocytes (top) and monocytes (bottom) from cultured Flt3⁺ ETPs from neonatal mice. Scale bars, 5 μ m. (h) Quantitative analysis of the expression of genes associated with lymphoid cells, myeloid cells and megakaryocytes-erythroid cells by purified Flt3⁺ ETPs from newborn mice ($n = 6$; 25 cells per replicate); results are presented relative to the expression of *Hprt* (encoding hypoxanthine guanine phosphoribosyl transferase). *, ≤ 0.001 (below detection limit). Data are representative of four experiments (a); fourteen experiments (c); seven (b) or sixteen (d) experiments (Flt3^{hi} ETPs); sixteen experiments (bone marrow; b); four experiments (Flt3⁻ ETPs (b) and other DN populations (b,d)); ten experiments (Flt3⁻ ETPs; d); one experiment (e); two to sixteen experiments (f); one experiment (g); or two experiments (h); mean and s.e.m. in b,d,f; average and s.d. of six replicates in h.)

progenitor can be generated in the passage from the bone marrow to the thymus and/or a thymic cell population with combined T cell, GM and B cell lineage potential can be identified among or beyond the ETPs. In the last scenario, the ETP could either be a lymphoid-GM-restricted multipotent progenitor or a pluripotent hematopoietic stem cell or progenitor cell that also has MkE potential. ETPs have been studied mostly in adult mice^{5,6,8,9}. However, thymic involution (the physiological shrinking of the thymus with age that occurs in all vertebrates) indicates that thymopoiesis, and therefore thymus seeding, is much more active in the early postnatal thymus¹⁸. The B cell potential of early thymocytes, at the population level, is much higher (although still low) in the neonatal thymus than in the adult thymus¹⁹. In agreement with published studies, lineage-negative (Lin^-) $\text{CD4}^-\text{CD8}\alpha^-\text{CD25}^-\text{c-Kit}^{\text{hi}}$ ETPs represented only 0.01% of adult thymocytes⁵, but as many as 40% of ETPs had cell-surface expression of the cytokine tyrosine kinase receptor Flt3, a greater frequency than reported before²⁰ (Fig. 1a). Also in agreement with published findings^{5,20}, a low but highly reproducible frequency of Flt3-expressing ETPs from adult mice generated B cells (3.5%–4.5%), whereas no other thymocyte progenitors from adult mice, including Flt3⁻ ETPs, had any detectable B cell potential (Fig. 1b and Supplementary Fig. 2). The frequency of $\text{Lin}^- \text{CD4}^-\text{CD8}\alpha^-\text{CD25}^-\text{c-Kit}^{\text{hi}}\text{Flt3}^{\text{hi}}$ ETPs was more than tenfold higher in newborn mice than in adult mice (Fig. 1c) and, most notably, the frequency of $\text{Lin}^- \text{CD4}^-\text{CD8}\alpha^-\text{CD25}^-\text{c-Kit}^{\text{hi}}\text{Flt3}^{\text{hi}}$ ETPs with B cell potential was 25% (Fig. 1d and Supplementary Fig. 3). Neither $\text{Lin}^- \text{CD4}^-\text{CD8}\alpha^-\text{CD25}^-\text{c-Kit}^{\text{hi}}\text{Flt3}^{\text{hi}}$ thymocytes nor downstream populations at $\text{CD4}^-\text{CD8}^-$ double-negative stages 2–4 (DN2–DN4) in the neonatal thymus had any B cell potential (Fig. 1d). $\text{Lin}^- \text{CD4}^-\text{CD8}\alpha^-\text{CD25}^-\text{c-Kit}^{\text{hi}}\text{Flt3}^{\text{hi}}$ ETPs from newborn mice also produced B cells *in vivo* when transplanted into irradiated mice deficient in recombination-activating gene 1 ($\text{Rag1}^{-/-}$) but produced only very low numbers of short-lived myeloid cells (Supplementary Fig. 4).

Because B cell activity in the thymus might reflect the presence of cells already committed to the B cell lineage^{21,22}, which overlap with the $\text{CD25}^-\text{CD44}^+$ phenotype of DN1 thymocytes, we did a fate-mapping experiment with mice expressing Cre recombinase from the promoter of the gene encoding the immunoglobulin-associated antigen

CD79A (*Cd79a*), in which all committed B cell progenitors and their progeny are labeled with enhanced yellow fluorescent protein^{23,24}. In agreement with published studies²³, cells of the B cell lineage, including all $\text{CD19}^+\text{B220}^+\text{CD43}^+\text{c-Kit}^+$ pro-B cells, as well as a fraction of Ly6D^+ CLPs ($\text{Lin}^- \text{CD19}^-\text{B220}^-\text{Sca-1}^{\text{lo}}\text{c-Kit}^{\text{lo}}\text{Flt3}^{\text{hi}}\text{IL-7R}\alpha^+\text{Ly6D}^+$), were labeled in the bone marrow (Supplementary Fig. 5a,b). We observed no cells expressing enhanced yellow fluorescent protein among $\text{Lin}^- \text{CD4}^-\text{CD8}\alpha^-\text{CD25}^-\text{c-Kit}^{\text{hi}}$ ETPs (Fig. 1e) or among Ly6D^+ CLPs ($\text{Lin}^- \text{CD19}^-\text{B220}^-\text{Sca-1}^{\text{lo}}\text{c-Kit}^{\text{lo}}\text{Flt3}^{\text{hi}}\text{IL-7R}\alpha^+\text{Ly6D}^-$) or LMPPs ($\text{Lin}^- \text{Sca-1}^+\text{c-Kit}^{\text{hi}}\text{Flt3}^{\text{hi}}$; Supplementary Fig. 5b,c).

In addition to producing B cells, $\text{Lin}^- \text{CD4}^-\text{CD8}\alpha^-\text{CD25}^-\text{c-Kit}^{\text{hi}}\text{Flt3}^{\text{hi}}$ ETPs from newborn mice gave rise efficiently to cells of the T cell, natural killer cell and GM lineages, as demonstrated before with ETPs from adult mice^{5,6,8,9} (Fig. 1f,g and Supplementary Fig. 6a). In contrast, ETPs from newborn mice were completely devoid of MkE potential (Fig. 1f). ETPs from adult mice lacked megakaryocyte potential as well but, in agreement with published studies^{8,9}, had GM potential (Supplementary Fig. 6a). Quantitative gene-expression analysis showed that purified $\text{Lin}^- \text{CD4}^-\text{CD8}\alpha^-\text{CD25}^-\text{c-Kit}^{\text{hi}}\text{Flt3}^{\text{hi}}$ ETPs from newborn mice expressed many genes associated with granulocytes-monocytes and lymphoid cells but not those associated with megakaryocytes or erythroid cells (Fig. 1h). Single-cell PCR showed that as many as 65% of newborn $\text{Lin}^- \text{CD4}^-\text{CD8}\alpha^-\text{CD25}^-\text{c-Kit}^{\text{hi}}\text{Flt3}^{\text{hi}}$ ETPs coexpressed genes of granulocytes-monocytes and lymphoid cells, whereas they lacked expression of genes of megakaryocytes and erythroid cells (Fig. 2a).

To establish whether the T cell, B cell and GM potential of ETPs from neonatal mice reflected the existence of a multipotent lymphomyeloid progenitor in the thymus or only a mixture of lineage-restricted progenitors, we assessed the combined lineage potential of single $\text{Lin}^- \text{CD4}^-\text{CD8}\alpha^-\text{CD25}^-\text{c-Kit}^{\text{hi}}\text{Flt3}^{\text{hi}}$ ETPs. We sorted single ETPs onto OP9 bone marrow stroma to allow each single ETP to proliferate for 54 h, after which we split the expanded cell cultures and transferred them for an additional week to OP9 stroma and OP9 stroma expressing the Notch ligand Delta-like 1 (OP9-DL1 stroma) to promote differentiation into B cells and combined differentiation into T cells and myeloid cells, respectively.

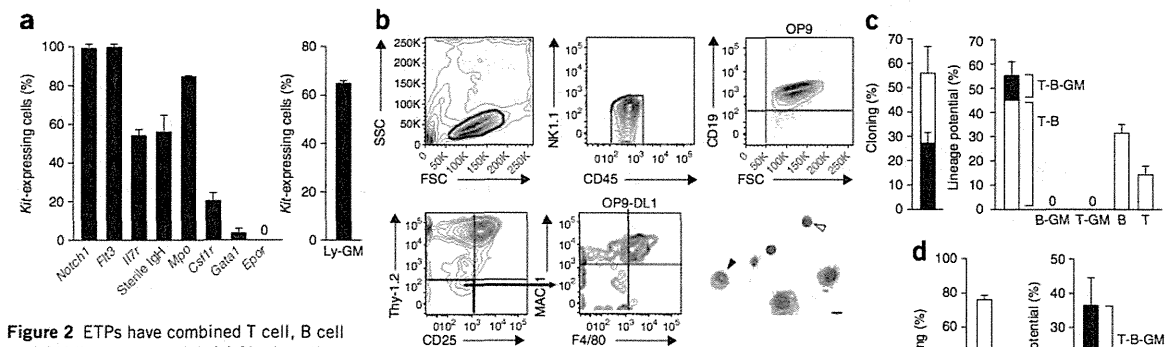


Figure 2 ETPs have combined T cell, B cell and GM lineage potential.

(a) Single-cell analysis of the expression of genes associated with lymphoid cells, myeloid cells and megakaryocytes-erythroid cells, by purified Flt3^{hi} ETPs from newborn mice, among cells that express *Kit* (left; 96–98% of total cells; $n = 176$ cells). Right, frequency of ETPs with combined lymphoid-GM gene expression based on coexpression (Ly-GM) of one or more genes of the lymphoid program (*Il7r* and *Sterile IgH*) and myeloid-GM program (*Csf1r* and *Mpo*) but not of the MkE program (*Gata1* and *Epor*). (b) Flow cytometry and morphology analysis of a clone from a single Flt3^{hi} ETP cell from a newborn wild-type mouse, with combined T cell–B cell (white arrowhead) and myeloid (black arrowhead) lineage potential. Scale bar, 5 μm . (c,d) Cloning frequency (left) of ETPs generating CD45⁺ cells (open bars) and CD45⁺ cells that are also positive for T cell, B cell and/or GM markers (filled bars), assessed for wild-type mice (c) or *vavP-Mcl1*-transgenic mice (d). Right, lineage distribution of clones from single ETPs from wild-type mice (c; $n = 132$ cells) or *vavP-Mcl1*-transgenic mice (d; $n = 167$ cells). Data are from two experiments (a,d) or three experiments (b,c; mean and s.d. in a and mean and s.e.m. in c,d).

Although the frequency of ETP-derived clones with detectable GM potential was lower than that of assays in which only the GM differentiation of ETPs was promoted (Fig. 1f), we demonstrated the existence of single $\text{Lin}^- \text{CD4}^- \text{CD8}\alpha^- \text{CD25}^- \text{c-Kit}^{\text{hi}} \text{Flt3}^{\text{hi}}$ ETPs with combined T cell, B cell and GM lineage potential (9.2% of clones with a lineage 'readout'; Fig. 2b,c and Supplementary Fig. 7a). In fact, we tracked all the GM potential from wild-type ETPs to cells that not only had T cell potential, as demonstrated before^{8,9}, but also had B cell lineage potential (Fig. 2c). Next we used ETPs purified from mice expressing *Mcl1* (encoding the antiapoptotic protein Mcl-1) from the *vavP* transgenic vector²⁵ to evaluate whether enhanced cell survival could better sustain short-lived myeloid cells in the assay for combined myeloid and T lymphoid development. Whereas the B cell potential in thymuses from neonatal *Mcl1*-transgenic mice remained restricted to $\text{Lin}^- \text{CD4}^- \text{CD8}\alpha^- \text{CD25}^- \text{c-Kit}^{\text{hi}} \text{Flt3}^{\text{hi}}$ ETPs (Supplementary Fig. 7c), the frequency of ETPs that generated combined T cell-B cell-GM progeny was 20% of all single ETPs (relative to 9.2% of wild-type ETPs) producing one or more hematopoietic lineages (Fig. 2d and Supplementary Fig. 7b). These findings obtained with single-cell clonal assays established the existence of thymic ETPs with combined T cell, B cell and GM lineage potential.

Lymphomyeloid ETPs are the most multipotent thymic progenitors

We next explored whether the $\text{Lin}^- \text{CD4}^- \text{CD8}\alpha^- \text{CD25}^- \text{c-Kit}^{\text{hi}} \text{Flt3}^{\text{hi}}$ ETPs with combined T cell, B cell and GM lineage potential

represented the most multipotent progenitors in the neonatal thymus. The lack of detectable MKE potential in $\text{Lin}^- \text{CD4}^- \text{CD8}\alpha^- \text{CD25}^- \text{c-Kit}^{\text{hi}} \text{Flt3}^{\text{hi}}$ ETPs did not rule out the possibility of the presence of rare pluripotent hematopoietic stem cells or progenitor cells in the neonatal thymus. Thus, we first used highly sensitive flow cytometry to investigate the expression of three antigens, CD150 (ref. 26), CD201 (ref. 27) and *Mpl*²⁸; each with high expression on most if not all HSCs as well as multipotent progenitors with sustained MKE potential. None of these antigens was expressed on $\text{Lin}^- \text{CD4}^- \text{CD8}\alpha^- \text{CD25}^- \text{c-Kit}^{\text{hi}}$ ETPs (Fig. 3a). Similar to a subfraction of bone marrow LMPPs, all ETPs expressed *Rag1*, as assessed through the use of a green fluorescent protein (GFP) reporter under control of the *Rag1* promoter²⁹, and most expressed the chemokine receptor CCR9 (Fig. 3b), in agreement with published studies of ETPs, LMPPs and CLPs from adult mice^{30,31}. No bone marrow HSCs expressed either the *Rag1*-driven GFP reporter or CCR9 (Fig. 3b).

Whole thymocytes from neonatal mice transplanted intravenously or intrafemorally (to bypass potential changes in bone marrow-homing properties after entry into the thymus) into irradiated wild-type mice transiently reconstituted T cells and small amounts of B cells (Fig. 3c,d) but failed to sustain any long-term multilineage reconstitution (Fig. 3e,f), in further support of the idea that the postnatal thymus does not contain any HSCs. To enhance the detection of HSCs potentially present in the thymus, we depleted whole-thymocyte samples of CD4^+ and CD8^+ cells and transplanted these into recipient mice intravenously or intrafemorally (Fig. 3g,h). The absence of long-term

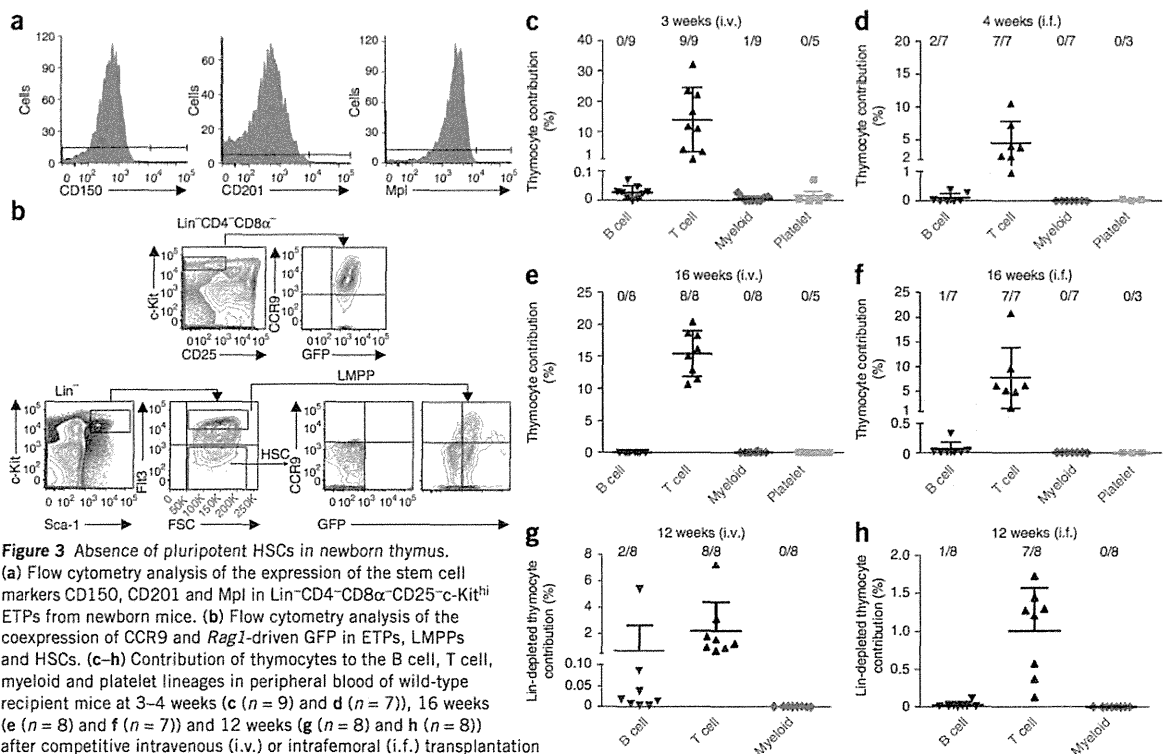


Figure 3 Absence of pluripotent HSCs in newborn thymus.

(a) Flow cytometry analysis of the expression of the stem cell markers CD150, CD201 and *Mpl* in $\text{Lin}^- \text{CD4}^- \text{CD8}\alpha^- \text{CD25}^- \text{c-Kit}^{\text{hi}} \text{Flt3}^{\text{hi}}$ ETPs from newborn mice. (b) Flow cytometry analysis of the coexpression of CCR9 and *Rag1*-driven GFP in ETPs, LMPPs and HSCs. (c–h) Contribution of thymocytes to the B cell, T cell, myeloid and platelet lineages in peripheral blood of wild-type recipient mice at 3–4 weeks (c ($n = 9$) and d ($n = 7$)), 16 weeks (e ($n = 8$) and f ($n = 7$)) and 12 weeks (g ($n = 8$) and h ($n = 8$)) after competitive intravenous (i.v.) or intrafemoral (i.f.) transplantation of total thymocytes (c–f) or of thymocyte samples depleted of CD4^+ and CD8^+ cells (Lin-depleted; g, h), from neonatal mice expressing eGFP driven by *Vwf* (in which all platelets express eGFP) or wild-type mice. Numbers at top indicate the frequency of reconstituted mice relative to total mice in group. Each symbol represents an individual mouse; horizontal lines indicate the mean (and s.d.). Data are representative of two experiments (a, b) or one experiment (c–h).

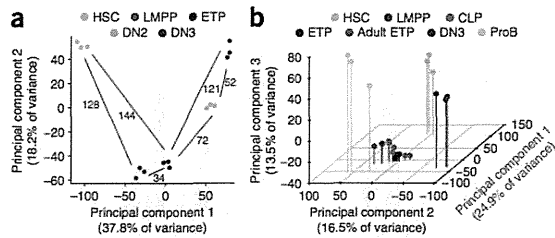


Figure 4 The gene expression of ETPs clusters closer to that of candidate TSPs in the bone marrow than to that of other thymic progenitors. Two- and three-dimensional principal-component analysis of normalized global gene-expression profiles of purified HSCs, IL-7R α^+ LMPPs, ETPs, DN2 cells and DN3 cells from neonatal mice (a; $n = 3$ replicates), and purified HSCs ($n = 3$ replicates), IL-7R α^+ LMPPs ($n = 3$ replicates), CLPs ($n = 4$ replicates), ETPs ($n = 3$ replicates), DN3 cells ($n = 3$ replicates) and pro-B cells ($n = 3$ replicates) from neonatal mice (b) and ETPs from adult mice (b; $n = 2$ replicates), with 1,600–2,000 cells per replicate. Each symbol represents an individual biological sample (sorted from a different pool of mice). Numbers adjacent to lines indicate Euclidean distances between average x and y values for each population measured in the first two principal components. Data are representative of three experiments (a) or two to three experiments (b).

myeloid reconstitution in all major hematopoietic organs, as well as the lack of thymocyte-derived T cell progenitors in the thymus after 13 weeks in all but one transplanted mouse, further confirmed the absence of pluripotent HSCs in the thymus (Fig. 3g,h and Supplementary Fig. 8a–d). Collectively, these results demonstrated the absence of HSCs in the postnatal thymus, a finding compatible with the proposal that ETPs with combined T cell, B cell and GM lineage potential are the most multipotent progenitors in the thymus.

ETPs are closely molecularly related to bone marrow TSPs

Because our findings indicated that Lin $^-$ CD4 $^-$ CD8 α^- CD25 $^-$ c-Kit hi Flt3 hi ETPs in the neonatal thymus had the same lineage potential as Lin $^-$ Sca-1 $^+$ c-Kit hi Flt3 hi LMPPs expressing the *Rag1*-driven GFP reporter (which also had high expression of interleukin 7 receptor α (IL-7R α); Supplementary Fig. 9a) in the bone marrow^{13,32}, we next investigated the molecular relationship between ETPs and IL-7R α^+ LMPPs and HSCs in the bone marrow of neonatal mice. We also compared ETPs with the next stages of lineage restriction in the thymus: Lin $^-$ CD44 $^+$ CD25 $^-$ c-Kit hi DN2 cells, which sustain combined T cell and GM lineage potential but no B cell lineage potential^{8,9}, and Lin $^-$ CD44 $^-$ CD25 $^+$ DN3 cells, which represent the first T cell-restricted progenitors in the thymus³³. Global gene-expression analysis done as described before³⁴, demonstrated that the gene-expression profile of ETPs clustered much closer to that of IL-7R α^+ LMPPs in the bone marrow than to that of thymic DN2 or DN3 progenitors or bone marrow HSCs. Moreover, the gene-expression profile of LMPPs clustered closer to that of ETPs than to that of HSCs, and that of DN2 cells was closer to that of DN3 cells than to that of ETPs (Fig. 4a). Because CLPs have been suggested to be candidate TSPs⁷ and have been shown to not only have lymphoid potential but also sustain some myeloid potential similar to LMPPs³⁵, we also compared the molecular profiles of ETPs with those of the two candidate TSP populations in the bone marrow: IL-7R α^+ LMPPs and Lin $^-$ CD19 $^-$ B220 $^-$ Sca-1 lo c-Kit lo Flt3 $^+$ IL-7R α^+ Ly6D $^-$ CLPs³⁶ (Fig. 4b). The molecular profiles of ETPs from neonatal mice clustered closely with those of CLPs as well as those of LMPPs and were more distant from those of HSCs, DN3 cells and also pro-B cells. Moreover, the molecular profiles of ETPs from neonatal and adult mice clustered closely together with those of LMPPs and CLPs (Fig. 4b). These findings established a close molecular relationship between Lin $^-$ CD4 $^-$ CD8 α^- CD25 $^-$ c-Kit hi Flt3 hi ETPs in

© 2012 Nature America, Inc. All rights reserved.

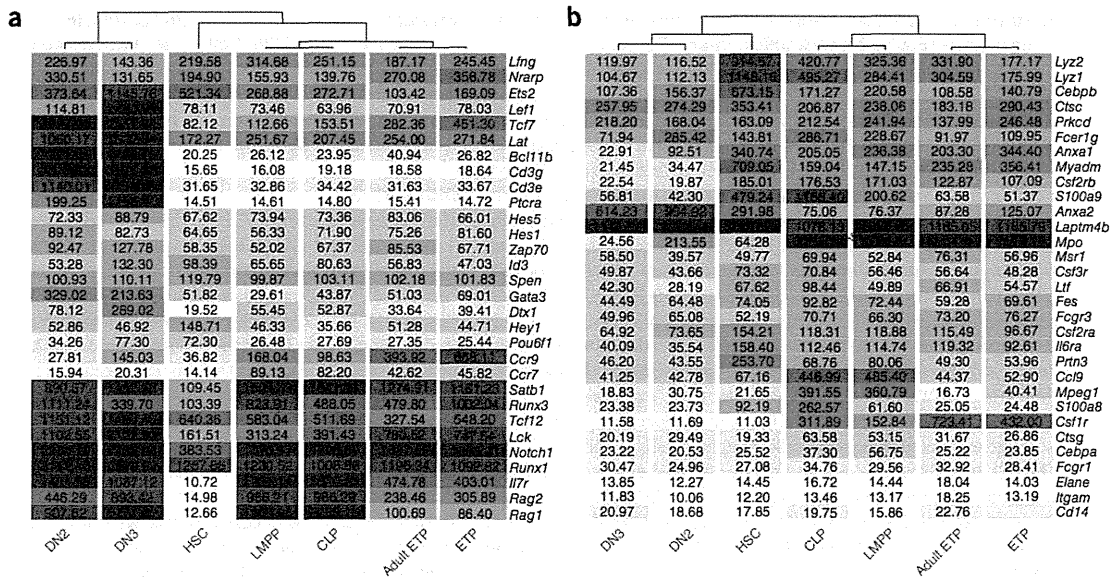


Figure 5 ETPs, IL-7R α^+ LMPPs and CLPs have closely related T cell- and myeloid-lineage transcriptional profiles. Expression of genes associated with the T cell lineage (a) or GM lineage (b) by purified HSCs ($n = 6$ replicates), IL-7R α^+ LMPPs ($n = 6$ replicates), CLPs ($n = 4$ replicates), ETPs ($n = 6$ replicates), DN2 cells ($n = 3$ replicates) and DN3 cells ($n = 6$ replicates) from neonatal mice, and ETPs from adult mice ($n = 2$ replicates), with 1,600–2,000 cells per replicate (derivation of gene lists, Online Methods and Supplementary Note). Numbers in boxes indicate normalized median values obtained by the robust multiarray average method; darker shading indicates higher expression; lighter shading indicates lower expression. Dendrograms above indicate relationships between samples according to their gene profiles. Data are representative of two to four experiments.

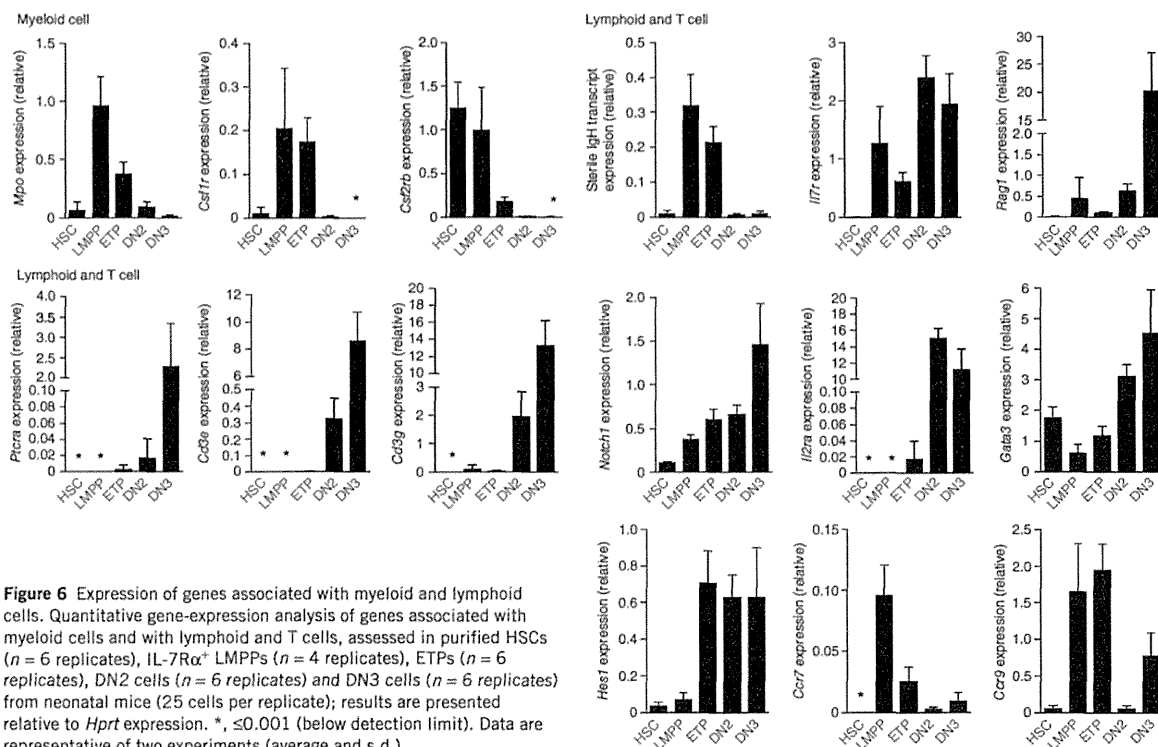


Figure 6 Expression of genes associated with myeloid and lymphoid cells. Quantitative gene-expression analysis of genes associated with myeloid cells and with lymphoid and T cells, assessed in purified HSCs ($n = 6$ replicates), IL-7R α^+ LMPPs ($n = 4$ replicates), ETPs ($n = 6$ replicates), DN2 cells ($n = 6$ replicates) and DN3 cells ($n = 6$ replicates) from neonatal mice (25 cells per replicate); results are presented relative to *Hprt* expression. *, ≤ 0.001 (below detection limit). Data are representative of two experiments (average and s.d.).

the thymus and candidate TSPs with lympho-myeloid potential in the bone marrow (Fig. 4a,b and Supplementary Fig. 9b,c).

To more specifically assess gene expression associated with the T cell and GM lineages, we derived lists of genes associated with T cells and granulocytes-monocytes from the literature and from published data sets^{37,38} (Supplementary Note). When we compared the programs associated with the T cell and GM lineages, we found that those of ETPs from adult and neonatal mice clustered closely for both the T cell and GM lineage, and closer to those for IL-7R α^+ LMPPs and CLPs than to those for DN2 or DN3 cells in the thymus or HSCs in the bone marrow (Fig. 5a,b and Supplementary Fig. 9d,e). Notably, many T cell-associated genes that eventually undergo considerable upregulation in DN2 cells and even further after T cell commitment of DN3 cells, had already been upregulated in LMPPs and CLPs, relative to their low expression in HSCs. There was less change in expression of these T cell-associated genes in LMPPs and CLPs relative to their expression in ETPs (Fig. 5a). By quantitative RT-PCR, we investigated in greater detail some genes related to myeloid cells, lymphoid cells, T cells and Notch (Fig. 6). In addition to confirming the combined expression of genes associated with the GM lineage (*Mpo*, *Csf1r* and *Csf2rb*) and lymphoid lineage (sterile IgH, *Il7r* and *Rag1*) in ETPs and LMPPs, these data also showed that characteristic early T cell-specific genes (*Ptcra*, *Cd3e* and *Cd3g*) were not significantly upregulated in either multipotent IL-7R α^+ LMPPs or ETPs. In contrast, *Notch1* was upregulated in LMPPs and even further upregulated in ETPs and, in agreement with that, the Notch target genes *Il2ra* (*Cd25*), *Gata3* and, in particular, *Hes1* (ref. 39) were upregulated in the transition from LMPPs to ETPs. Finally, whereas HSCs lacked expression of *Ccr7* and *Ccr9*, which encode chemokine receptors critical for migration to the thymus^{30,31}, these genes showed

considerable upregulation in IL-7R α^+ LMPPs, in further support of the idea that LMPPs are TSPs. Collectively, these results demonstrated that ETPs and candidate TSPs such as LMPPs and CLPs had closely related gene-expression profiles, which reinforced the proposal that ETPs are more probably derived from lympho-myeloid-restricted TSPs than from HSCs in the bone marrow.

DISCUSSION

Here we have identified ETPs in the neonatal thymus with combined T cell, B cell and GM lineage potential but no MkE lineage potential, and we have demonstrated a close functional and molecular link between ETPs and candidate TSPs in the bone marrow. The observation that ETPs lacked MkE potential was notable for reconciliation of the ongoing debate about the roadmap for commitment to different hematopoietic lineages, as the classical model for such commitment indicates that the first lineage-commitment step of HSCs results in strict separation of the myeloerythroid- and lymphoid-commitment pathways^{1,14}. According to that model, any cell with combined lymphoid and GM potential should also have MkE potential. However, we found that Lin⁻CD4⁻CD8 α ⁻CD25⁻c-Kit^{hi}Flt3^{hi} ETPs with combined T cell, B cell and GM lineage potential were devoid of megakaryocyte or erythroid lineage potential. These cells coexpressed, at the single-cell level, genes related to lymphoid cells and granulocytes-monocytes, but not megakaryocytes or erythroid cells, similar to LMPPs with identical lineage potentials in the bone marrow^{13,32,34}. Thus, our study has provided further support for a myeloid-based lineage-commitment model^{2,13,15-17} by demonstrating the existence of T cell-B cell-GM-restricted progenitors in the postnatal thymus. Such cells have been identified before in the bone marrow and fetal liver^{13,34}.

The real frequency of Lin⁻CD4⁻CD8 α ⁻CD25⁻c-Kit^{hi}Flt3^{hi} ETPs from neonatal mice with T cell–B cell–GM potential is probably higher than we were able to demonstrate. Analysis of clones grown from single ETPs from newborn mice demonstrated that most ETPs with T cell potential simultaneously had B cell potential, but less than 20% of these also showed GM potential in wild-type mice, although under optimized GM conditions more than 50% of ETPs demonstrated GM potential. We speculated that the lower detection of cells of the GM lineages in the multilineage clonal assay reflected the short lifespan of vulnerable myeloid cells, and in agreement with that, transgenic expression of the antiapoptotic protein Mcl-1 enhanced the generation of myeloid cells from ETPs with combined T cell, B cell and GM potential in neonatal mice, most probably through the enhanced survival of myeloid cells. Our findings also suggest that the T cell–B cell–GM restricted progenitor identified is the most multipotent progenitor in the neonatal thymus, as we did not detect any M κ E lineage potential or M κ E-specific gene expression among highly purified ETPs. Furthermore, we also demonstrated that there were no phenotypic or *in vivo* reconstituting HSCs or multipotent progenitors in the neonatal thymus.

Published studies have suggested that the earliest fetal thymic progenitors in the embryo have combined T cell and myeloid lineage potential but no B cell lineage potential^{10,11}, which raises the possibility that the progenitors that seed the embryonic thymus might be distinct from and more committed than those in the postnatal thymus. In contrast to the seeding of the neonatal thymus, which was the focus of our study, it remains unclear if the adult thymus is also seeded with ETPs with combined T cell, GM and B cell lineage potential. As thymopoiesis is much less active in adult thymus than in newborn thymus, it can be predicted that the most multipotent ETPs are much more infrequent in adult thymus than in the neonatal thymus. Although the low frequency of B cell lineage potential of ETPs from adult mice reported before^{6,20} and confirmed here does not allow definitive demonstration of the combined T cell, GM and B cell lineage potentials of ETPs from adult mice with the present clonal lineage-potential assay, it is notable that rare Lin⁻CD4⁻CD8 α ⁻CD25⁻c-Kit^{hi}Flt3^{hi} ETPs were the only thymocytes from adult mice with B cell potential. In addition, we found that ETPs from adult mice, like ETPs from neonatal mice, had GM potential but not megakaryocyte potential, and global gene-expression analysis indicated a close molecular relationship between ETPs from neonatal mice and those from adult mice. Collectively, these data suggest that the adult thymus, like neonatal thymus, might also be seeded by rare T cell–B cell–GM progenitors, which we were unequivocally able to identify in neonatal thymus. Nevertheless, there are distinct differences among HSCs and hematopoietic progenitor cells from fetal, neonatal and adult mice. The regulated migration of TSPs to the thymus might also differ in the fetus, newborn and adult, so it remains possible that the lineage potentials of TSPs from embryos, newborns and adults might be different.

Although our studies have established the extent of ETP multipotentiality (T cell–B cell–GM) and the close phenotypic and molecular relationship of ETPs, LMPPs and CLPs with the same lineage potentials in the bone marrow^{13,32,34,35}, they do not exclude the possibility that other candidate progenitors in the bone marrow might seed the thymus⁴⁰. A published study has suggested that T cell–GM–restricted progenitors might exist in the bone marrow⁴¹, although such progenitors remain to be purified and characterized in further detail. The GM potential of ETPs is limited, and studies have suggested that it has little if any functional relevance to these progenitors' acting as myeloid progenitors in the thymus^{35,42}.

Likewise, it seems unlikely that ETPs have any important physiological role as B cell progenitors. Instead, the importance of these sustained lineage potentials of ETPs is to provide a better understanding of the lineage-restriction steps required for lineage commitment from pluripotent HSC in the bone marrow to a T cell–restricted progenitor in the thymus. Specifically, progenitors with combined T cell–B cell–GM potential, such as LMPPs and CLPs, are derived in the bone marrow from HSCs that have shut down the M κ E transcriptional programs and lineage potential. Unlike HSCs, LMPPs and CLPs upregulate CCR9, which enables their transfer to the thymus^{30,31}. Migration to the thymus seems critical for the next T cell lineage–restriction steps, first to a T cell–GM progenitor^{8,9} and finally to a fully T cell–restricted progenitor.

Our studies have provided new insight into the normal stepwise process of commitment to the T cell lineage in the bone marrow and thymus. In addition, they are also relevant to the clinically, phenotypically and molecularly distinct group of mixed T cell–GM acute lymphoblastic leukemias that are mostly observed in children but also seen in adults, called 'ETP leukemias'⁴³. Furthermore, the sustained B cell potential of ETPs might explain why the MLL–AF4 fusion oncogene that is highly specific for human B cell malignancies can give rise to B cell malignancies even if targeted to thymic progenitors⁴⁴.

METHODS

Methods and any associated references are available in the online version of the paper at <http://www.nature.com/natureimmunology/>.

Accession code. GEO: microarray data, GSE29382.

Note. Supplementary information is available on the Nature Immunology website.

ACKNOWLEDGMENTS

We thank N. Sakaguchi (Kumamoto University) for mice with *Rag1*-driven GFP expression; T. Graf (Center for Genomic Regulation) for mice with expression of enhanced GFP (eGFP) driven by the gene encoding lysozyme M κ ; S. Cory (Walter and Eliza Hall Institute of Medical Research) for vavP-*Mcl1*-transgenic mice; M. Reth (Max Planck Institute of Immunobiology) for Cd79a^{tm1(Cre)Reth} mice; S. Srinivas (University of Oxford) for mice expressing enhanced yellow fluorescent protein from the *Rosa26* locus; A. Cumano (Institut Pasteur) for OP9 and OP9-DL1 stromal cells; Biomedical Services at Oxford University for animal support; S. Clark, T. Furey and B. Wu for technical assistance; and E. Zuo and M. Eckart at the Stanford Protein and Nucleic Acid Facility for gene array services. Supported by the Medical Research Council, UK (H4RPLK0 to S.E.W.J.) and EU-FP7 EuroSysTem Integrated projects to S.E.W.J., C.B. and A.F.), Leukaemia and Lymphoma Research (C.B., A.F. and A.J.M.), the Crafoord Foundation (A.H.), The George Danielsson Foundation (A.H.) and Swedish Society for Medicine and Swedish Cancer Foundation (A.H.).

AUTHOR CONTRIBUTIONS

S.E.W.J. and S.L. designed and conceived of the overall research, analyzed the data and wrote the manuscript, which was subsequently reviewed and approved by all authors; J.B. processed RNA samples; I.C.M. and S.S. analyzed the microarray data; A.J.M., D.A. and A.H. did quantitative and single-cell PCR; A.J.M., S.M. and K.A. did morphology analyses; H.F., S.L. and M.L. sorted cells by flow cytometry; S.L., M.L., T.B.-J., S.D., N.B.-V., H.B., T.C.L., A.D. and S.J.L. contributed to flow cytometry and *in vitro* culture experiments; S.L., S.D., N.B.-V., P.S.W., T.C.L. and H.B. did *in vivo* transplantations; T.E. provided assistance in the design and analysis of microarray experiments; C.B., A.F., R.P., M.d.B., I.G. and T.M. contributed advice and input on experimental design; and C.N., A.S.-P. and C.C. generated and provided input on studies of mice expressing eGFP driven by *Vwf* (encoding the von Willebrand factor homolog).

COMPETING FINANCIAL INTERESTS

The authors declare no competing financial interests.

Published online at <http://www.nature.com/natureimmunology/>.

Reprints and permissions information is available online at <http://www.nature.com/reprints/index.html>.



1. Reya, T., Morrison, S.J., Clarke, M.F. & Weissman, I.L. Stem cells, cancer, and cancer stem cells. *Nature* **414**, 105–111 (2001).
2. Katsura, Y. Redefinition of lymphoid progenitors. *Nat. Rev. Immunol.* **2**, 127–132 (2002).
3. Donskoy, E. & Goldschneider, I. Thymocytopoiesis is maintained by blood-borne precursors throughout postnatal life. A study in parabiotic mice. *J. Immunol.* **148**, 1604–1612 (1992).
4. Scollay, R., Smith, J. & Stauffer, V. Dynamics of early T cells: prothymocyte migration and proliferation in the adult mouse thymus. *Immunol. Rev.* **91**, 129–157 (1986).
5. Allman, D. *et al.* Thymopoiesis independent of common lymphoid progenitors. *Nat. Immunol.* **4**, 168–174 (2003).
6. Benz, C. & Bleul, C.C. A multipotent precursor in the thymus maps to the branching point of the T versus B lineage decision. *J. Exp. Med.* **202**, 21–31 (2005).
7. Bhandoola, A., von Boehmer, H., Petrie, H.T. & Zuniga-Pflucker, J.C. Commitment and developmental potential of extrathymic and intrathymic T cell precursors: plenty to choose from. *Immunity* **26**, 678–689 (2007).
8. Wada, H. *et al.* Adult T-cell progenitors retain myeloid potential. *Nature* **452**, 768–772 (2008).
9. Bell, J.J. & Bhandoola, A. The earliest thymic progenitors for T cells possess myeloid lineage potential. *Nature* **452**, 764–767 (2008).
10. Desanti, G.E. *et al.* Clonal analysis reveals uniformity in the molecular profile and lineage potential of CCR9⁺ and CCR9⁻ thymus-settling progenitors. *J. Immunol.* **186**, 5227–5235. [10.4049/jimmunol.1002686](https://doi.org/10.4049/jimmunol.1002686) (2011).
11. Masuda, K. *et al.* Thymic anlage is colonized by progenitors restricted to T, NK, and dendritic cell lineages. *J. Immunol.* **174**, 2525–2532 (2005).
12. Kondo, M., Weissman, I.L. & Akashi, K. Identification of clonogenic common lymphoid progenitors in mouse bone marrow. *Cell* **91**, 661–672 (1997).
13. Adolfsson, J. *et al.* Identification of Flt3⁺ lympho-myeloid stem cells lacking erythromegakaryocytic potential: a revised road map for adult blood lineage commitment. *Cell* **121**, 295–306 (2005).
14. Orkin, S.H. & Zon, L.I. Hematopoiesis: an evolving paradigm for stem cell biology. *Cell* **132**, 631–644 (2008).
15. Luc, S., Buza-Vidas, N. & Jacobsen, S.E. Delineating the cellular pathways of hematopoietic lineage commitment. *Semin. Immunol.* **20**, 213–220 (2008).
16. Doulatov, S. *et al.* Revised map of the human progenitor hierarchy shows the origin of macrophages and dendritic cells in early lymphoid development. *Nat. Immunol.* **11**, 585–593 (2010).
17. Goardon, N. *et al.* Coexistence of LMPP-like and GMP-like leukemia stem cells in acute myeloid leukemia. *Cancer Cell* **19**, 138–152 (2011).
18. Taub, D.D. & Longo, D.L. Insights into thymic aging and regeneration. *Immunol. Rev.* **205**, 72–93 (2005).
19. Ceredig, R., Bosco, N. & Rolink, A.G. The B lineage potential of thymus settling progenitors is critically dependent on mouse age. *Eur. J. Immunol.* **37**, 830–837 (2007).
20. Sambandam, A. *et al.* Notch signaling controls the generation and differentiation of early T lineage progenitors. *Nat. Immunol.* **6**, 663–670 (2005).
21. Radtke, F. *et al.* Deficient T cell fate specification in mice with an induced inactivation of Notch1. *Immunity* **10**, 547–558 (1999).
22. Feyerabend, T.B. *et al.* Deletion of Notch1 converts pro-T cells to dendritic cells and promotes thymic B cells by cell-extrinsic and cell-intrinsic mechanisms. *Immunity* **30**, 67–79 (2009).
23. Hobeika, E. *et al.* Testing gene function early in the B cell lineage in mb1-cre mice. *Proc. Natl. Acad. Sci. USA* **103**, 13789–13794 (2006).
24. Srinivas, S. *et al.* Cre reporter strains produced by targeted insertion of EYFP and ECFP into the ROSA26 locus. *BMC Dev. Biol.* **1**, 4 (2001).
25. Campbell, K.J. *et al.* Elevated Mcl-1 perturbs lymphopoiesis, promotes transformation of hematopoietic stem/progenitor cells, and enhances drug resistance. *Blood* **116**, 3197–3207 (2010).
26. Kiel, M.J. *et al.* SLAM family receptors distinguish hematopoietic stem and progenitor cells and reveal endothelial niches for stem cells. *Cell* **121**, 1109–1121 (2005).
27. Balazs, A.B., Fabian, A.J., Esmon, C.T. & Mulligan, R.C. Endothelial protein C receptor (CD201) explicitly identifies hematopoietic stem cells in murine bone marrow. *Blood* **107**, 2317–2321 (2006).
28. Solar, G.P. *et al.* Role of c-mpl in early hematopoiesis. *Blood* **92**, 4–10 (1998).
29. Igarashi, H., Gregory, S.C., Yokota, T., Sakaguchi, N. & Kincade, P.W. Transcription from the RAG1 locus marks the earliest lymphocyte progenitors in bone marrow. *Immunity* **17**, 117–130 (2002).
30. Zlotoff, D.A. *et al.* CCR7 and CCR9 together recruit hematopoietic progenitors to the adult thymus. *Blood* **115**, 1897–1905 (2010).
31. Krueger, A., Willenzon, S., Lyszkiewicz, M., Kremmer, E. & Forster, R. CC chemokine receptor (CCR) 7 and 9 double-deficient hematopoietic progenitors are severely impaired in seeding the adult thymus. *Blood* **115**, 1906–1912 (2010).
32. Luc, S. *et al.* Downregulation of Mpl marks the transition to lymphoid-primed multipotent progenitors with gradual loss of granulocyte-monocyte potential. *Blood* **111**, 3424–3434 (2008).
33. Godfrey, D.I., Kennedy, J., Suda, T. & Zlotnik, A. A developmental pathway involving four phenotypically and functionally distinct subsets of CD3⁺CD4⁺CD8⁻ triple-negative adult mouse thymocytes defined by CD44 and CD25 expression. *J. Immunol.* **150**, 4244–4252 (1993).
34. Mansson, R. *et al.* Molecular evidence for hierarchical transcriptional lineage priming in fetal and adult stem cells and multipotent progenitors. *Immunity* **26**, 407–419 (2007).
35. Ehrlich, L.I., Serwold, T. & Weissman, I.L. In vitro assays misrepresent in vivo lineage potentials of murine lymphoid progenitors. *Blood* **117**, 2618–2624 (2011).
36. Inlay, M.A. *et al.* Ly6d marks the earliest stage of B-cell specification and identifies the branchpoint between B-cell and T-cell development. *Genes Dev.* **23**, 2376–2381 (2009).
37. Pronk, C.J.H. *et al.* Elucidation of the phenotypic, functional, and molecular topography of a myeloerythroid progenitor cell hierarchy. *Cell Stem Cell* **1**, 428–442 (2007).
38. David-Fung, E.S. *et al.* Transcription factor expression dynamics of early T-lymphocyte specification and commitment. *Dev. Biol.* **325**, 444–467 (2009).
39. Wendorf, A.A. *et al.* Hes1 is a critical but context-dependent mediator of canonical Notch signaling in lymphocyte development and transformation. *Immunity* **33**, 671–684 (2010).
40. Petrie, H.T. & Kincade, P.W. Many roads, one destination for T cell progenitors. *J. Exp. Med.* **202**, 11–13 (2005).
41. Chi, A.W. *et al.* Identification of Flt3CD150 myeloid progenitors in adult mouse bone marrow that harbor T lymphoid developmental potential. *Blood* **118**, 2723–2732 (2011).
42. Schlenner, S.M. *et al.* Fate mapping reveals separate origins of T cells and myeloid lineages in the thymus. *Immunity* **32**, 426–436 (2010).
43. Coustan-Smith, E. *et al.* Early T-cell precursor leukaemia: a subtype of very high-risk acute lymphoblastic leukaemia. *Lancet Oncol.* **10**, 147–156 (2009).
44. Metzler, M. *et al.* A conditional model of MLL-AF4 B-cell tumorigenesis using invertebrate technology. *Oncogene* **25**, 3093–3103 (2006).